Atmos. Chem. Phys. Discuss., 11, 19395–19442, 2011
www.atmos-chem-phys-discuss.net/11/19395/2011/
doi:10.5194/acpd-11-19395-2011

Atmospheric Chemistry and Physics Discussions

Sources of carbonaceous aerosols and deposited black carbon in the Arctic in winter–spring: implications for radiative forcing

Q. Wang[1], D. J. Jacob[1], J. A. Fisher[1], J. Mao[1], E. M. Leibensperger[1], C. C. Carouge[1], P. Le Sager[1], Y. Kondo[2], J. L. Jimenez[3], M. J. Cubison[3], and S. J. Doherty[4]

[1]School of Engineering and Applied Sciences and Department of Earth and Planetary Sciences, Harvard University, Cambridge, Massachusetts, USA
[2]Department of Earth and Planetary Science, Graduate school of Science, University of Tokyo, Tokyo, Japan
[3]Cooperative Institute for Research in the Environmental Sciences and Department of Chemistry and Biochemistry, University of Colorado, Boulder, Colorado, USA

[4]Joint Institute for the Study of Atmosphere and Ocean, 3737 Brooklyn Ave NE, Seattle, Washington, USA

Received: 22 June 2011 – Accepted: 23 June 2011 – Published: 6 July 2011

Correspondence to: Q. Wang (wang2@fas.harvard.edu)

Published by Copernicus Publications on behalf of the European Geosciences Union.

ACPD
11, 19395–19442, 2011

Abstract

We use a global chemical transport model (GEOS-Chem CTM) to interpret observations of black carbon (BC) and organic aerosol (OA) from the NASA ARCTAS aircraft campaign over the North American Arctic in April 2008, together with longer-term records in surface air and in snow. We find that Russian open fires were the dominant source of OA in the troposphere during ARCTAS but that BC was more of anthropogenic origin, particularly in surface air. This source attribution is confirmed by correlation of BC and OA with acetonitrile and sulfate in the model and in the observations. Asian emissions are the main anthropogenic source of BC in the free troposphere but European, Russian and North American sources are also important in surface air. Russian anthropogenic emissions appear to dominate the Arctic source of BC in surface air in winter. Open fire influences on Arctic surface BC in spring are much higher in the Eurasian than in the North American sector. Most of the BC transported to the Arctic in the lower troposphere is deposited within the Arctic, in contrast to the BC transported at higher altitudes. Pan-Arctic 2007–2009 observations of BC concentrations in snow are well reproduced by the model, with maximum values in the Russian Arctic and much lower values in the North American Arctic. We find that anthropogenic sources contribute 90% of BC deposited to Arctic snow in January–March and 57% in April–May 2007–2009. The mean decrease in Arctic snow albedo from BC deposition is estimated to be 0.6% in spring 2007–2009, resulting in a regional surface radiative forcing consistent with previous estimates.

1 Introduction

Aerosol pollution in the Arctic peaks in winter–spring, when transport from mid-latitudes is most intense and removal by deposition is slow (Barrie et al., 1981; Quinn et al., 2002, 2007; Law and Stohl, 2007). The principal submicron aerosol components are sulfate and organic aerosols (OA) (Ricard et al., 2002; Zhang et al., 2007), which affect

ACPD
11, 19395–19442, 2011

Arctic climate by scattering solar radiation and modifying cloud properties (Kristjansson et al., 2005; Koch et al., 2007; Quinn et al., 2007, 2008). Black carbon (BC) is only a minor contributor to aerosol mass but is of great climatic concern as an absorber of solar radiation both in the atmosphere (Jacobson, 2001; Koch et al., 2007; Quinn et al., 2008) and after deposition to snow (Warren and Wiscombe, 1985; Flanner et al., 2007; McConnell et al., 2007; Quinn et al., 2008). Here we use a global chemical transport model (GEOS-Chem CTM) to interpret aircraft observations of BC and OA from the NASA ARCTAS campaign over the North American Arctic in April 2008 (Jacob et al., 2010), together with longer-term records of BC observations at surface sites and in snow. Our goal is to better understand the factors controlling the concentrations of carbonaceous aerosols in the Arctic, the deposition of BC to snow, and the implications for snow albedo and associated radiative forcing.

Historical observations of elevated BC at surface sites in the Arctic have been attributed to fossil fuel combustion in Northern Europe and Russia, based on air flow back-trajectories and correlations with trace metal tracers (Shaw, 1982; Djupstrom et al., 1993). BC concentrations decreased from the 1980s to 2000, followed by a slight increase in the past decade (Sharma et al., 2006; Eleftheriadis et al., 2009; Gong et al., 2010; Hirdman et al., 2010). Recent measurements of BC in Arctic snow show a strong association with biomass burning based on tracer correlations and optical properties (Hegg et al., 2009; Doherty et al., 2010; Hegg et al., 2010). Stohl et al. (2007) reported an event of extremely high BC concentrations in the Arctic in spring associated with agricultural burning in Eastern Europe.

The origin of OA in the Arctic has received far less attention. A two-year record of OA concentrations in Northern Finland shows a minimum in winter and a maximum in summer attributed to biogenic and photochemical sources (Ricard et al., 2002). Measurements at Barrow show maximum OA in winter–spring, and correlations with chemical tracers suggest a dominance of ocean emissions (winter) and combustion sources (spring) (Shaw et al., 2010; Frossard et al., 2011).

ACPD
11, 19395–19442, 2011

Surface measurements of aerosols are not representative of the troposphere, particularly in the Arctic because of strong stratification (Klonecki et al., 2003). The vertical distribution of aerosols has important implications for radiative forcing (Koch et al., 2009a). Two coordinated aircraft campaigns with carbonaceous aerosol measurements were conducted in April 2008 out of Fairbanks, Alaska: the NASA Arctic Research of the Composition of the Troposphere from Aircraft and Satellites (ARCTAS) (Jacob et al., 2010) and the NOAA Aerosol, Radiation and Cloud Processes affecting Arctic Climate (ARCPAC) (Brock et al., 2011). These two campaigns provided extensive vertical profiling of trace gases and speciated aerosols through the depth of the Arctic troposphere. They showed in particular large enhancements of carbonaceous aerosols in the mid-troposphere due to open fires in Russia and Kazakhstan (Warneke et al., 2009, 2010; Spackman et al., 2010; Kondo et al., 2011; Matsui et al., 2011; McNaughton et al., 2011).

A number of CTM studies have investigated the sources of BC in the Arctic, but there are large disagreements among models and discrepancies with observations (Shindell et al., 2008; Koch et al., 2009b; Tilmes et al., 2011). Emissions in East Asia have been growing and some work has pointed out an impact on winter–spring Arctic BC concentrations, especially in the free troposphere (Koch and Hansen, 2005; Shindell et al., 2008; Tilmes et al., 2011). Stohl (2006) found little wintertime Asian influence over the Arctic either at the surface or in the free troposphere. There has been far less attention to modeling OA over the Arctic, but open fires would be expected to be a dominant source (Koch et al., 2007).

Here we use the GEOS-Chem CTM to simulate observations of BC and OA from the DC-8 aircraft in ARCTAS, including correlations with other species, and to link the aircraft data with longer-term measurements in surface air and snow. We first evaluate the model with BC observations in northern mid-latitudes source regions to test the emission inventories. We then apply the model to diagnose the sources of BC and OA in the ARCTAS aircraft data, in surface air observations, and (for BC) in 2007–2009 Arctic snow. From there we infer the radiative forcing from BC deposited to

ACPD
11, 19395–19442, 2011

Arctic snow. This work builds on previous studies that applied GEOS-Chem to simulate observations of other species over the Arctic during ARCTAS/ARCPAC including CO (Fisher et al., 2010), sulfate-ammonium aerosols (Fisher et al., 2011), HO_x radicals (Mao et al., 2010), and mercury (Holmes et al., 2010).

2 Model description

We use the GEOS-Chem CTM version 8-01-04 (http://geos-chem.org) driven by assimilated meteorological data from the Goddard Earth Observing System (GEOS-5) of the NASA Global Modeling and Assimilation Office (GMAO). The GEOS-5 data have 6-h temporal resolution (3-h for surface quantities and mixing depths), 47 vertical layers, and $0.5^\circ \times 0.667^\circ$ horizontal resolution. We degrade the horizontal resolution to $2^\circ \times 2.5^\circ$ for input to GEOS-Chem. We initialize the model with a one-month spin-up followed by simulation of January–May 2008.

The simulation of carbonaceous aerosols in GEOS-Chem is as described by Park et al. (2006) and Fu et al. (2009), with modifications of wet deposition and emission inventories described below. BC and primary OA (POA) are emitted by combustion. Secondary OA (SOA) is produced in the atmosphere by reversible condensation of oxidation products of biogenic and aromatic volatile organic compounds (Chung and Seinfeld, 2002; Henze and Seinfeld, 2006; Henze et al., 2008), as well as by irreversible condensation of glyoxal and methylglyoxal (Fu et al., 2008, 2009). We find that SOA formed by either of these pathways is negligible in the winter–spring Arctic and we do not discuss it further here. The simulations of BC and POA in GEOS-Chem are linear (concentrations are proportional to sources) and we isolate the contributions from different sources by tagging them in the model.

Dry deposition in GEOS-Chem follows a standard resistance-in-series scheme (Wesely, 1989) as implemented by Wang et al. (1998). The global annual mean dry deposition velocity is $0.1\,\mathrm{cm\,s^{-1}}$ for BC and OA, typical of current models (Reddy and Boucher, 2004; Huang et al., 2010a). We impose an aerosol dry deposition velocity

ACPD
11, 19395–19442, 2011

of 0.03 cm s^{-1} over snow and ice based on eddy-covariance flux measurements in the Arctic by Nilsson and Rannik (2001) and Held et al. (2011).

2.1 Wet depostion

Proper representation of scavenging by cold clouds and snow is important for simulation of aerosols in the Arctic. The standard scheme for aerosol scavenging in GEOS-Chem described by Liu et al. (2001) includes scavenging in convective updrafts, as well as in-cloud and below-cloud scavenging from convective and large-scale precipitation. Liu et al. (2001) do not distinguish between scavenging by rain and snow. Here we introduce such a distinction as well as other improvements to the scavenging scheme.

In the standard GEOS-Chem model, below-cloud scavenging (washout) is calculated using a washout rate constant $S = aR$, where R is the precipitation rate (mm h^{-1}) and $a = 0.1$ mm $^{-1}$ is a washout coefficient obtained by integrating scavenging efficiencies from impaction, interception, and diffusion over typical raindrop and aerosol size distributions (Dana and Hales, 1976). This overestimates integrated scavenging during a precipitation event because it does not account for the preferential removal of very fine and coarse particles, shifting the aerosol size distribution toward the more scavenging-resistant accumulation mode (Feng, 2007, 2009; Croft et al., 2009). We improve it here by using the parameterization $S = aR^b$ constructed by Feng (2007, 2009) for individual aerosol modes (nucleation, accumulation, and coarse) and for snow as well as rain. We adopt their accumulation-mode scavenging coefficients for all aerosols except dust and sea salt, for which we adopt their coarse-mode coefficients. The corresponding values for rain ($T \geq 268$ K) are $a = 1.1 \times 10^{-3}$ mm $^{-1}$ and $b = 0.61$ for accumulation-mode aerosols, and $a = 0.92$ mm $^{-1}$ and $b = 0.79$ for coarse-mode aerosols; for snow ($T < 268$ K), they are $a = 2.8 \times 10^{-2}$ mm $^{-1}$ and $b = 0.96$ for accumulation-mode aerosols, and $a = 1.57$ mm $^{-1}$ and $b = 0.96$ for coarse-mode aerosols. Scavenging of accumulation-mode aerosols by snow is an order of magnitude more efficient than by rain because of the larger areal cross section of snow

ACPD
11, 19395–19442, 2011

crystals (Murakami et al., 1983).

In-cloud scavenging (rainout) efficiently removes aerosols serving as cloud condensation nuclei (CCN) or ice nuclei (IN). In the case of warm and mixed-phase clouds ($T > 258$ K), we assume 100% incorporation of hydrophilic aerosols in the cloud droplets followed by efficient scavenging when liquid water is converted to precipitation by coalescence or riming. We assume that 80% of BC and 50% of POA are emitted as hydrophobic (Cooke et al., 1999; Park et al., 2003), and convert them to hydrophilic in the atmosphere with an e-folding time of 1 day which yields a good simulation of BC export efficiency in continental outflow (Park et al., 2005). In the case of cold clouds ($T < 258$ K), we assume that only dust and hydrophobic BC can serve as IN and hence be removed by scavenging (Chen et al., 1998; Andreae and Rosenfeld, 2008), with the acknowledgment that cold-cloud aerosol scavenging is highly uncertain (Karcher et al., 2007; Baumgardner et al., 2008; Cozic et al., 2008; Targino et al., 2009).

Precipitation is a subgrid process on the horizontal scale of GEOS-Chem. A critical variable in the wet deposition parameterization is the areal fraction F_k of a grid box at vertical model layer k that actually experiences precipitation. Liu et al. (2001) applied the formulation of Giorgi and Chameides (1986) for the areal fraction F'_k over which new precipitation is formed:

$$F'_k = \frac{Q_k}{LC_1} \tag{1}$$

where Q_k is the grid-scale formation rate of new precipitation (kg m^{-3} s^{-1}), L is the condensed water content of the precipitating cloud and is assumed to be constant ($L = 1.0 \times 10^{-3}$ kg m^{-3}) (DelGenio et al., 1996), and C_1 is the rate constant for conversion of cloud water to precipitation ($C_1 = C_{1\min} + Q_k/L$ with $C_{1\min} = 1.0 \times 10^{-4}$ s^{-1}). The algorithm is initiated for each grid square at the top of the tropospheric column and proceeds downward, computing the actual precipitating fraction F_k in layer k (index decreasing downward) as $F_k = \max(F'_k, F_{k+1})$ to account for precipitation formation overhead. In previous versions of GEOS-Chem, $Q_k > 0$ caused rainout to be applied to

ACPD
11, 19395–19442, 2011

the whole precipitation area fraction F_k and washout was only applied when $F_k > 0$ and $Q_k \leq 0$ (negative Q_k indicating net evaporation). This caused an overestimation of in-cloud scavenging and underestimation of below-cloud scavenging, as $F_{k+1} > F'_k$ should be an indication of washout taking place over the fractional area $F_{k+1} - F'_k$ of layer k. In our present simulation, we apply rainout in layer k to the precipitating fraction F'_k and washout to the additional fractional area $F_{\text{diff}} = \max(0,\ F_{k+1} - F'_k)$. The correction slows aerosol scavenging as washout is generally less efficient than rainout. The global lifetime of carbonaceous aerosols in our simulation is 6 days, within the range of 5–11 days from current models (Koch et al., 2009b).

Model transport of BC from northern mid-latitudes to the Arctic is highly sensitive to assumptions about scavenging efficiency. Liu et al. (2011) found in their AM-3 model a factor of 100 increase in winter–spring Arctic BC, and better agreement with observations from surface sites and from ARCTAS, by using a photochemically-varying timescale for BC hydrophobic-to-hydrophilic aging (up to 1–2 weeks in winter) and reducing deposition efficiencies relative to their original model. They found in their model that 30–50% of Arctic BC remained hydrophobic in winter. However, TRACE-P aircraft observations in Asian outflow in March–April provide good constraints that the BC aging time scale is no more than 2 days (Park et al., 2005), and aircraft observations of light absorption in ARCTAS implied significant coating for the BC particles (McNaughton et al., 2011).

2.2 Emissions of BC and OA

Figure 1 shows the hemispheric emissions of BC and POA (primary organic aerosol) in April 2008 in the model. Table 1 gives regional and global annual totals for 2008. The source regions are chosen to encompass the bulk of Northern Hemisphere emissions. Anthropogenic emissions (fossil fuel and biofuel combustion) are from Bond et al. (2007) for 2000, but with doubled emissions in Russia and Asia (including China, India, Korea and Japan) for both BC and POA to match BC surface observations in China and in the Arctic as discussed below. This doubling would be consistent with the

ACPD
11, 19395–19442, 2011

strong recovery of the Russian economy since 2000 (IEA, 2010) and with the general increase in Chinese emissions over the past decade (Zhang et al., 2008a; Lu et al., 2010).

April 2008 saw exceptionally high forest and agricultural fire activity in Russia and Kazahkstan (hereafter referred to collectively as "Russia") (Warneke et al., 2009; Fisher et al., 2010) as well as typical seasonal fire activity in Southeast Asia (including India and Southern China). We specify open fire emissions with the Fire Locating and Monitoring of Burning Emissions (FLAMBE) inventory (Reid et al., 2009), which has $1^\circ \times 1^\circ$ spatial resolution and hourly temporal resolution based on MODIS and GOES satellite fire counts. The FLAMBE inventory provides fine particle ($PM_{2.5}$) emissions based on total estimated fuel combustion, carbon fraction in the fuel, and $PM_{2.5}$ emission factors (Reid et al., 2005, 2009). We partition $PM_{2.5}$ emissions into BC and OA using emission factors from Andreae and Merlet (2001) for different vegetation types. Fisher et al. (2010) previously used FLAMBE to simulate ARCTAS/ARCPAC CO observations with GEOS-Chem and found that Russian and Southeast Asian emissions needed to be reduced to 53% and 45%, respectively. We apply here the same reductions to BC and OA emissions. Open fires in Russia were the dominant source of OA in ARCTAS (Warneke et al., 2009, 2010), and we find from tagged source attribution that OA emissions from Russian fires must be reduced by an additional 36% to match the ARCTAS observations. This defines our OA emission factor from the fires, given below.

To define the BC emission factor from the Russian fires we use observations of the BC/OA concentration ratio in fire plumes. Warneke et al. (2009) reported BC/OA ratios of 0.14 (agricultural fires) and 0.15 (forest fires) on a carbon basis for Russian fire plumes sampled in ARCPAC, and we find a similar observed ratio of 0.12 ± 0.03 for fire plumes sampled in ARCTAS (Fig. 2). A BC/OA emission ratio in the model of 0.13 from fires reproduces these values in the fire plumes. The resulting emission factors for Russian fires used in the model are $0.87\,g\,kg^{-1}$ (gram carbon per kilogram dry mass burned) for BC and $6.8\,g\,kg^{-1}$ for OA, consistent with the values of 0.30–0.82 and 2.0–9.7 reported in the literature (Andreae and Merlet, 2001; Akagi et al., 2011).

ACPD
11, 19395–19442, 2011

Figure 3 compares annual mean surface air concentrations of BC in the model in 2008 with observations from networks in the US (2008), China (2006), and Europe (2002–2003). Our objective is to diagnose any large model bias in these three major source regions relevant to the Arctic. For the US we use 2008 data from the rural IMPROVE network (http://vista.cira.colostate.edu/improve/Data/IMPROVE/AsciiData.aspx). For China and Europe we do not have network observations for 2008, and use therefore data for other years with the assumption that interannual variability is small: Zhang et al. (2008b) for rural/regional sites in China in 2006, and the BC/OC campaign in Europe in 2002–2003 (http://tarantula.nilu.no/projects/ccc/emepdata.html). We diagnose for each region the normalized mean bias:

$$\mathrm{NMB} = 100\% \times \sum_i (M_i - O_i) / \sum_i O_i \quad (2)$$

where the sum is over the ensemble of sites i, and M_i and O_i are the modeled and observed values, respectively.

The data in Fig. 3 show normalized mean biases of −24% for China, −31% for Europe, and +35% for the US. Without doubling the inventory from Bond et al. (2007) the bias for China would be much larger (NMB = −61%). Underestimation in Europe is mainly due to three sites in Northern Italy and Belgium. Without these three sites the NMB would decrease to −0.7%. The overestimation of BC in the US can be explained by a 40% decrease in observed concentrations between 2000 (year of the Bond et al. (2007) inventory) and 2008, as shown by Leibensperger et al. (2011).

3 Sources of BC and OA in the Arctic

3.1 Constraints from aircraft data

Figure 4 shows the DC-8 flight tracks in ARCTAS. BC was measured with a SP2 (Single Particle Soot Photometer) instrument (Kondo et al., 2011). OA and other aerosol information were measured by an Aerosol Mass Spectrometer (AMS) (Jimenez et al.,

ACPD
11, 19395–19442, 2011

2003) for sub-micrometer particles, which we assume account for the bulk of OA. The AMS measures OA in units of $\mu g\,m^{-3}$ and we convert this to $\mu g\,C\,m^{-3}$ with a ratio of 2.1 typical of nonurban aerosols (Turpin and Lim, 2001; Aiken et al., 2008). The model is sampled along the flight tracks at the same time and location as the observations, and the aircraft data are averaged over the GEOS-Chem grid. Observations outside the Arctic (south of 60° N), in the stratosphere ($[O_3]/[CO] > 1.25\,mol\,mol^{-1}$), and in fire plumes ($[CH_3CN] > 200$ ppt) are excluded. We previously used the information from fire plumes to constrain the BC emission factor (Sect. 2).

BC and OA were measured from the ARCPAC aircraft concurrently with ARCTAS, but for fewer flights and a much smaller spatial domain around Fairbanks. Fisher et al. (2011) previously compared the GEOS-Chem sulfate-ammonium aerosol simulation to the ensemble of ARCTAS and ARCPAC observations, and found the ARCPAC data difficult to interpret because of the limited sampling and focus on fire plumes. We limit here our use of the ARCPAC data to the constraints that they provide on biomass burning emission factors (Warneke et al., 2009, 2010) and BC deposition (Spackman et al., 2010).

Figure 5 shows the overall fine aerosol composition measured by the ARCTAS DC-8 in 2-km altitude bins, providing context for the relative importance of BC and OA. Sea salt and dust are excluded as only bulk measurements were made in ARCTAS and we expect their coarse-mode fractions to be dominant. OA and sulfate are the dominant components of the fine aerosol. Sulfate is dominant in surface air but OA becomes comparable in the free troposphere, because sulfate shows little variation with altitude while OA is strongly peaked at 2–6 km.

Figure 6 shows scatterplots of simulated vs. observed BC and OA concentrations during ARCTAS, and Fig. 7 shows mean vertical profiles. The model has some success in reproducing the variability of the individual observations, with a correlation coefficient $r = 0.65$ for BC and 0.62 for OA. There are some large underestimates in the mid-troposphere associated with elevated CH_3CN, a tracer of biomass burning, but these may reflect the inability of the model to resolve fine plumes not screened by the

ACPD
11, 19395–19442, 2011

[CH_3CN] < 200 ppt filter. Eulerian models such as GEOS-Chem cannot resolve fine structures (Rastigejev et al., 2010). Concentrations of BC average 53 ± 109 ng C m^{-3} in the observations and 63 ± 65 ng C m^{-3} in the model. Concentrations of OA average 0.40 ± 0.56 µg C m^{-3} in the observations and 0.35 ± 0.37 µg C m^{-3} in the model.

The model successfully reproduces the mean vertical distributions of BC and OA, with peaks in the mid-troposphere. Model source attribution in Fig. 7 shows that these peaks are due to Russian fires, and in the case of BC also to Asian anthropogenic influence. Fires contribute 46% of BC and 84% of OA at 2–6 km altitude in the model. The mid-tropospheric maximum reflects the lifting of Russian fire and Asian pollution effluents by warm conveyor belts (WCBs) originating from the Pacific Rim of the Asian continent (Liu et al., 2003; Stohl, 2006; Fisher et al., 2010). The strong influence of open fires at 2–6 km is consistent with the observed strong correlations of BC vs. CH_3CN ($r = 0.74$) and OA vs. CH_3CN ($r = 0.81$) and has been reported in previous ARCTAS/ARCPAC analyses (Warneke et al., 2009, 2010; Spackman et al., 2010; Kondo et al., 2011; Matsui et al., 2011).

We find that open fires are the dominant source of OA at all altitudes in the model, but anthropogenic sources are more important for BC and completely dominate near the surface (Fig. 7). We evaluate this source attribution by using observed and simulated correlations with sulfate, an aerosol tracer of anthropogenic influence. Simulated GEOS-Chem sulfate is from Fisher et al. (2011). Figure 8 shows observed and simulated scatterplots of BC and OA vs. sulfate, indicating good agreement in the correlation coefficients and the slopes of the regression lines at 2–6 km (mid-troposphere) and 0–1 km (near-surface). There is significant correlation between OA and sulfate in the mid-troposphere, consistent with the well-known mixing of pollution and fire influences in Asian outflow lifted by WCBs (Bey et al., 2001) and previously documented in ARCTAS and ARCPAC (Fisher et al., 2010; Brock et al., 2011). Figure 8 shows a population of points at altitude > 6 km with extremely high sulfate concentrations (> 3 µg m^{-3} STP) and low BC and OA concentrations, corresponding to a plume transported from East Asia as indicated by back-trajectories. The strong enrichment of sulfate relative to

ACPD
11, 19395–19442, 2011

carbonaceous aerosols in that plume is consistent with Asian pollution having experienced wet scavenging, as previously shown by van Donkelaar et al. (2008) and Dunlea et al. (2009) in observations from the INTEX-B aircraft campaign.

The contribution of open fire emissions in the model decreases from the mid-troposphere to near-surface air (<1 km), where it accounts for 20% of BC and 60% of OA. The concentration ratios relative to sulfate are also much lower in near-surface air than in the mid-troposphere, both in the model and in observations (Fig. 8). This is consistent with Fisher et al. (2011), who found a major contribution to Arctic boundary layer sulfate from boundary layer transport of European and North American pollution, in contrast to the mid-troposphere where Asian pollution dominates. This boundary layer anthropogenic influence, adding to the subsidence from the mid-troposphere, is far more important for BC than for OA because of the much higher BC/OA emission ratio from anthropogenic sources than from open fires (Table 1). Consequently, the observed ratio of BC vs. OA increases from 0.17 in the mid-troposphere to 0.26 near the surface (Fig. 9), and this is also well captured in the model.

Our estimation of the open fire contribution to BC along the ARCTAS DC-8 flight tracks agrees with the value of 33–41% reported by McNaughton et al. (2011) using CH_3CN and the OA/sulfate ratio to classify the data. Matsui et al. (2011) attributed most of the BC measured in ARCTAS to Russian fire emissions using CH_3CN and dichloromethane (CH_2Cl_2) to classify the data, but their analysis focused on plumes and ignored background air.

Broader examination of model results over the scale of the Arctic polar cap (north of 60° N) in April 2008 indicates that open fire emissions contribute 50% of total BC in the Arctic tropospheric column and 81% of total OA. Fire influences are the strongest in the Eurasian Arctic (not sampled by the aircraft). Asian pollution dominates the source of anthropogenic BC in the Arctic tropospheric column, but less so in surface air which is most relevant for BC deposition to snow (Shindell et al., 2008; Huang et al., 2010b). Our model Asian contribution to Arctic BC in spring is higher than previous studies (Koch and Hansen, 2005; Shindell et al., 2008; Tilmes et al., 2011). This reflects

ACPD
11, 19395–19442, 2011

our higher Asian emission inventory, constrained by observations at Chinese sites as discussed in Sect. 2.

3.2 Surface observations

We now turn to surface observations in Jan-May 2008 to provide broader seasonal context. Figure 10 compares model results with monthly average surface concentrations observed in Alaska at Denali (low Arctic) and Barrow (high Arctic) in 2002–2008 (locations shown in Fig. 4). Model contributions from different sources are shown. Observations at Denali are from the IMPROVE network (http://vista.cira.colostate.edu/improve/Data/IMPROVE/AsciiData.aspx) using a thermal/optical reflectance method. Observations at Barrow are from the NOAA Global Monitoring Division (http://www.esrl.noaa.gov/gmd/aero/net/), reported as aerosol light absorption coefficients from a particle soot absorption photometer. We use a mass absorption efficiency of 9.5 $m^2\ g^{-1}$ to convert the absorption coefficients to BC mass concentrations based on ARCTAS data (McNaughton et al., 2011). OA observations at Barrow are from Shaw et al. (2010), who reported seasonal mean concentrations for March 2008–March 2009.

We find that the BC and OA observations at the surface sites in April 2008 are roughly consistent with the mean near-surface ARCTAS data (Fig. 7), but are more affected by Russian fires. The fire influence at Denali is larger than that at Barrow. Observations in April 2008 were anomalously high relative to the 2002–2008 April mean (thin lines in Fig. 9), which reflects the anomalously large Russian fires (Fisher et al., 2010).

Observations of BC at Barrow show higher values in winter (January–March) than spring (April–May), even in 2008. In contrast, Denali shows higher values in spring even in the 2002–2008 mean. The model fails to reproduce the seasonal variation at Denali, apparently because it overestimates local pollution influence from nearby Anchorage in winter. It is more successful at Barrow, although this is contingent on doubling of the Russian anthropogenic source from the Bond et al. (2007) inventory as described above. The winter maximum at Barrow is explained in the model by

ACPD
11, 19395–19442, 2011

the Russian anthropogenic source, transported to the North American Arctic in the boundary layer around the Siberian High with little dilution and little precipitation. This Russian source influence declines sharply in spring due to vertical mixing and to the weakening of the Siberian High. Sharma et al. (2006) found similar source attribution for BC at Barrow using back-trajectory analysis, and Fisher et al. (2011) found similar results for sulfate at Barrow using GEOS-Chem.

Observed OA at Denali shows similar winter–spring seasonality as BC. Our model reproduces this seasonality without the spurious local influence from Anchorage seen for BC (the OA/BC emission ratio from Anchorage in the Bond et al. (2007) inventory is 50% lower than the anthropogenic mean). Observations of OA at Barrow show little seasonal variation between winter and spring, which is consistent with the model as the decline in the Russian anthropogenic source from winter to spring is compensated by the open fire influence. Both at Denali and at Barrow, we find that we can largely explain the wintertime OA on the basis of anthropogenic sources and the springtime OA on the basis of open fires. The source attribution in spring is consistent with the work of Shaw et al. (2010) and Frossard et al. (2011), who identified a dominant combustion source for OA at Barrow on the basis of correlations with combustion tracers. But Shaw et al. (2010) also attributed most OA at Barrow in winter to oceanic emissions, which are not included here.

4 BC deposition in the Arctic and implications for radiative forcing

BC transported to the Arctic can either be removed by deposition or eventually ventilated out. We find in model sensitivity simulations that BC transported to the Arctic below 2 km is mostly deposited within the Arctic, whereas BC transported to the Arctic at higher altitudes is mostly ventilated out. Deposition is mainly by wet processes (90%). Spackman et al. (2010) inferred a dry deposition flux for BC of 170–1700 ng m^{-2} day^{-1} over snow/ice during ARCPAC on the basis of observed BC depletion in the boundary layer. Our computed dry deposition flux in the Western Arctic (mostly covered by

ACPD
11, 19395–19442, 2011

snow/ice) is about 1500 ng m^{-2} day^{-1} in spring, consistent with that estimate.

Figure 11 shows the spatial distribution of model BC deposition in winter (January–March) and spring (April–May) 2008, separately for open fire and anthropogenic contributions. Maximum deposition is in the Eurasian sector due to Russian and European anthropogenic sources, augmented in spring by Russian fires. The fires double BC deposition to the Arctic in spring relative to winter. The Asian anthropogenic contribution to BC deposition is very small in winter compared to European and Russian sources but becomes comparable to these sources in the spring.

While ARCTAS data only provide information for the North American Arctic, we find that the largest BC deposition flux to the Arctic is in the Eurasian sector with a dominant contribution from open fires during spring 2008 (Fig. 11). Doherty et al. (2010) reported snow BC concentrations from a large network of both Russian and North American Arctic sites in March–May 2007–2009. We compared these observations (available for download at http://www.atmos.washington.edu/sootinsnow/) to model values for the corresponding years, using the GFEDv2 fire inventory for 2007 (van der Werf et al., 2006) and the FLAMBE inventory with above scaling factors for 2009. MODIS fire counts show that spring 2007 had lower-than-average Russian fires while 2009 was near average, offering a contrast to spring 2008 which had anomalously high Russian fire activity (Fisher et al. (2010); http://disc.sci.gsfc.nasa.gov/giovanni/). The total model BC deposition to the Arctic in April–May is 16 Gg $month^{-1}$ for 2007 (including 13% from open fires), 41 Gg $month^{-1}$ for 2008 (61%), and 34 Gg $month^{-1}$ for 2009 (46%). Deposition in January–March has little interannual variability (14–19 Gg $month^{-1}$).

Figure 12 shows model results for the BC content of snow in winter (January–March) and spring (April–May) 2007–2009, as calculated from the ratio of BC to water deposition fluxes. The Doherty et al. (2010) sampling locations are indicated by purple circles. Model values are much higher over the Eurasian than the North American Arctic. There is relatively little variability over the Arctic Ocean. Low values over Greenland reflect the elevated surface. The mean BC snow content over the scale of the Arctic shows only

ACPD
11, 19395–19442, 2011

weak interannual variability in winter (12–15 ng g^{-1}) but large interannual variability in spring (13–38 ng g^{-1}), reflecting the open fire influence as discussed above.

Figure 13 shows scatterplots of simulated vs. observed BC content in snow for the Doherty et al. (2010) sites in the North American and Russian Arctic sectors. Observations are averaged over the model grid squares and the model is sampled for the month and year of observations. Model and observations in the North American Arctic sector generally agree within a factor of 2. Excluding the outlier with observed value of 30 ng g^{-1} in 2007, we find a good correlation between observations and the model with $r = 0.60$. Mean values are 11 ± 4 ng g^{-1} in the observations and 11 ± 3 ng g^{-1} in the model. Rough agreement between model and observations is also found in the Russian Arctic sector, with mean values of 31 ± 11 ng g^{-1} in the model and 23 ± 16 ng g^{-1} in the observations. The model indicates a dominant anthropogenic influence over Western Russia in 2007 and a dominant open fire influence over Eastern Russia in 2008, consistent with the analysis by Doherty et al. (2010).

Model source attribution shows that the mean contribution of open fires to the BC content in Arctic snow is 10% in winter and 65% in spring 2008 (43% for springs 2007–2009). It is dominant in the Russian Arctic sector in spring 2008 and in the Western Russian Arctic sector in spring 2009. Hegg et al. (2009, 2010) and Doherty et al. (2010) previously reported a dominant influence from biomass burning in their BC snow content data, based on absorption Ångstrom exponents and correlation with biomass burning tracers. Part of the discrepancy could reflect biofuel combustion, which accounts in the model for 38% of annual anthropogenic emissions in Asia and 25% in Russia, and would be highest in winter–spring due to residential heating. In addition, mixing of anthropogenic and fire influences in Asian outflow discussed above complicates source attribution in the observations; this mixing is apparent in the Hegg et al. (2010) analysis as an association of sulfate with biomass burning influence.

Figure 14 shows model results for the decreases in snow albedo in winter (January–March) and spring (April–May) 2008 due to BC deposition to snow. We assume a constant snow grain radius of 100 µm (McConnell et al., 2007) with no significant aging,

ACPD
11, 19395–19442, 2011

and estimate the effect of BC on snow albedo based on Fig. 2 in Warren and Wiscombe (1995). The resulting decrease in snow albedo averaged over the Arctic is 0.4% in winter and 0.8% in spring 2008 (0.6% for spring 2007–2009), lower than previous estimates of 1.1–4.7% (Park et al., 2005; Flanner et al., 2007; Koch et al., 2009a). By convolving this result with the GEOS-5 incoming solar radiation at the surface we deduce a radiative forcing over the Arctic (north of 60° N) from deposited BC of 0.1 W m^{-2} in winter and 1.7 W m^{-2} in spring 2008 (1.2 W m^{-2} for spring 2007–2009, including 0.6 W m^{-2} from anthropogenic sources only). A previous model calculation by Flanner et al. (2007) reported a radiative forcing of 0.02 W m^{-2} in winter and 0.53 W m^{-2} in spring due to anthropogenic BC over the same domain, similar to our values. The global annual mean radiative forcing due to the snow-albedo effect from anthropogenic BC is 0.13 W m^{-2} in our simulation, with a maximum in China (similar to the distribution described in Flanner et al., 2007). This is within the range estimated by the IPCC (0.1 ± 0.1 W m^{-2}) (Forster et al., 2007).

5 Conclusions

We used the GEOS-Chem chemical transport model (CTM) to interpret aircraft observations of black carbon (BC) and organic aerosol (OA) from the NASA ARCTAS campaign over the North American Arctic in April 2008, together with longer-term observations of BC concentrations in surface air and 2007–2009 pan-Arctic observations of BC snow content. Our focus was to quantify the contributions of different source types and source regions to Arctic BC and OA concentrations in winter–spring, the role of deposition processes, the resulting source attribution for BC in snow, and the implications for radiative forcing.

Our GEOS-Chem simulation includes an improved representation of aerosol scavenging by cold clouds and by snow, anthropogenic emissions of BC and OA from the Bond et al. (2007) inventory for 2000, and open fire emissions from the FLAMBE inventory of Reid et al. (2009) with hourly resolution. We evaluated BC sources from

ACPD
11, 19395–19442, 2011

the northern mid-latitude continents with data from observation networks. We find that Russian and Asian anthropogenic emissions have to be doubled from Bond et al. (2007) to improve the match to observations for BC, as might be expected from increasing fuel use in these regions since 2000. Unusually large fires occurred in Russia in April 2008. FLAMBE estimates of biomass burned for these fires had to be decreased as previously shown by Fisher et al. (2010) from ARCTAS and satellite CO data. We find that BC and OA fire emission factors of 0.87 and 6.8 g carbon per kg dry mass burned, respectively, give a good simulation of observed Russian fire plumes.

The resulting model provides a good fit to the mean observed concentrations and vertical gradients of BC and OA along the ARCTAS flight tracks. Open fires account for most of OA in the model while anthropogenic emissions are more important for BC. Model and observations show strong peaks in the mid-troposphere for both BC and OA, reflecting the transport of Russian fire and Asian anthropogenic effluents lifted by warm conveyor belts (WCBs). Open fires contribute 46% of BC and 84% of OA in the mid-troposphere (2–6 km) in the model. Near the surface (<1 km), by contrast, we find that fires contribute only 20% of BC and 60% of OA. Anthropogenic BC concentrations in the mid-troposphere are mostly of Asian anthropogenic origin, but in surface air we find comparable contributions from North America and Europe. These model source attributions are consistent with observed correlations of BC and OA with acetonitrile (a tracer of biomass burning) and with comparisons of simulated and observed correlations of BC and OA vs. sulfate. The dominant influence of open fire emissions on OA agrees with the previous work of Warneke et al. (2009, 2010). The much smaller contribution from open fires to ARCTAS BC is consistent with the previous work of McNaughton et al. (2011) but not with that of Warneke et al. (2010) and Matsui et al. (2011) who we argue gave excessive consideration to fire plumes.

Expanding the model results to the scale of the Arctic polar cap in April 2008 indicates that open fire emissions contribute 50% of total BC in the Arctic tropospheric column and 81% of total OA. We find the strongest fire influences in the Eurasian Arctic, with the highest BC and OA concentrations there. Asian pollution dominates the

ACPD
11, 19395–19442, 2011

source of anthropogenic BC in the Arctic tropospheric column, but less so in surface air which is most relevant for BC deposition to snow (Shindell et al., 2008; Huang et al., 2010b). Our relatively higher model Asian contribution to Arctic BC in spring compared with previous studies (Koch and Hansen, 2005; Shindell et al., 2008; Tilmes et al., 2011) reflects our higher Asian emission inventory, constrained by observations at Chinese sites.

We used surface air observations of BC and OA at two Alaskan sites (Denali and Barrow) in January–May 2002–2008 to place the aircraft data in a seasonal context. BC concentrations and model source attributions for April 2008 are consistent between the surface sites and the aircraft. The Denali site shows an increase of BC from winter to spring due to Russian fire and Asian pollution influences. The seasonality is reversed at Barrow with a winter maximum that we attribute to transport from Russia. A similar seasonal transition in source influence on BC at Barrow has been reported by Sharma et al. (2006) based on back-trajectory analyses. OA concentrations at Denali and Barrow are well simulated by the model, with similar sources as for BC, but with stronger impact of fire emissions in spring that dampens the seasonality at Barrow.

Spring 2008 was anomalously affected by Russian fires. We conducted simulations for January–May 2007–2009 to obtain an interannual perspective on BC deposition to the Arctic and to evaluate the model with a pan-Arctic network of observations of BC snow content (Doherty et al., 2010). We find in the model that the total BC deposition flux to the Arctic in 2007–2009 averages 17 (14–19) Gg month^{-1} in January–March and 30 (16–41) Gg month^{-1} in April–May, where the range indicates the interannual variability. Open fires contribute much more to BC deposition in the Eurasian Arctic than in the North American Arctic. The model reproduces well the observations of BC snow content and their variability, with highest values in the Russian Arctic and lowest in Greenland. In the model, anthropogenic sources account on average for 10% of BC content in the Arctic snow in January–March and 43% in April–May 2007–2009. Hegg et al. (2009, 2010) and Doherty et al. (2010) previously found a dominant biomass burning influence at most of their Arctic sites on the basis of correlations with tracers

ACPD
11, 19395–19442, 2011

and absorption Ångstrom exponents. Some of that influence could reflect biofuel use (38% of annual BC anthropogenic emissions in Asia according to Bond et al., 2007). Mixing of anthropogenic and fire influences also complicates source attribution in the observations.

We estimate deceases in snow albedo due to BC deposition in 2007–2009 to be 0.4% in winter and 0.6% in spring. The resulting mean surface radiative forcing over the Arctic in spring is 1.2 W m^{-2} (including open fires) and 0.6 W m^{-2} (anthropogenic only). This is consistent with the anthropogenic value of 0.53 W m^{-2} previously reported by Flanner et al. (2007) for the same region. Averaged over the global scale, we find an annual mean surface radiative forcing of 0.13 W m^{-2} from BC deposited to snow, within the range reported in IPCC 2007 (Forster et al., 2007).

Acknowledgements. This work was funded by the Decadal and Regional Climate Prediction using Earth System Models (EaSM) Program of the US National Science Foundation. MJC and JLJ were supported by NASA grant NNX08AD39G.

References

Aiken, A. C., DeCarlo, P. F., Kroll, J. H., Worsnop, D. R., Huffman, J. A., Docherty, K. S., Ulbrich, I. M., Mohr, C., Kimmel, J. R., Sueper, D., Sun, Y., Zhang, Q., Trimborn, A., Northway, M., Ziemann, P. J., Canagaratna, M. R., Onasch, T. B., Alfarra, M. R., Prevot, A. S. H., Dommen, J., Duplissy, J., Metzger, A., Baltensperger, U., and Jimenez, J. L.: O/C and OM/OC ratios of primary, secondary, and ambient organic aerosols with high-resolution time-of-flight aerosol mass spectrometry, Environ. Sci. Technol., 42, 4478–4485, doi:10.1021/es703009q, 2008.

Akagi, S. K., Yokelson, R. J., Wiedinmyer, C., Alvarado, M. J., Reid, J. S., Karl, T., Crounse, J. D., and Wennberg, P. O.: Emission factors for open and domestic biomass burning for use in atmospheric models, Atmos. Chem. Phys., 11, 4039–4072, doi:10.5194/acp-11-4039-2011, 2011.

Andreae, M. O. and Merlet, P.: Emission of trace gases and aerosols from biomass burning, Global Biogeochem. Cy., 15, 955–966, 2001.

ACPD
11, 19395–19442, 2011

Andreae, M. O. and Rosenfeld, D.: Aerosol-cloud-precipitation interactions – Part 1: The nature and sources of cloud-active aerosols, Earth-Sci. Rev., 89, 13–41, doi:10.1016/j.earscirev.2008.03.001, 2008.

Barrie, L. A., Hoff, R. M., and Daggupaty, S. M.: The influence of mid-latitudinal pollution sources on haze in the canadian arctic, Atmos. Environ., 15, 1407–1419, 1981.

Baumgardner, D., Subramanian, R., Twohy, C., Stith, J., and Kok, G.: Scavenging of black carbon by ice crystals over the Northern Pacific, Geophys. Res. Lett., 35, L22815, doi:10.1029/2008GL035764, 2008.

Bey, I., Jacob, D. J., Logan, J. A., and Yantosca, R. M.: Asian chemical outflow to the Pacific in spring: origins, pathways, and budgets, J. Geophys. Res.-Atmos., 106, 23097–23113, 2001.

Bond, T. C., Bhardwaj, E., Dong, R., Jogani, R., Jung, S. K., Roden, C., Streets, D. G., and Trautmann, N. M.: Historical emissions of black and organic carbon aerosol from energy-related combustion, 1850–2000, Global Biogeochem. Cy., 21, Gb2018, doi:10.1029/2006GB002840, 2007.

Brock, C. A., Cozic, J., Bahreini, R., Froyd, K. D., Middlebrook, A. M., McComiskey, A., Brioude, J., Cooper, O. R., Stohl, A., Aikin, K. C., de Gouw, J. A., Fahey, D. W., Ferrare, R. A., Gao, R.-S., Gore, W., Holloway, J. S., Hübler, G., Jefferson, A., Lack, D. A., Lance, S., Moore, R. H., Murphy, D. M., Nenes, A., Novelli, P. C., Nowak, J. B., Ogren, J. A., Peischl, J., Pierce, R. B., Pilewskie, P., Quinn, P. K., Ryerson, T. B., Schmidt, K. S., Schwarz, J. P., Sodemann, H., Spackman, J. R., Stark, H., Thomson, D. S., Thornberry, T., Veres, P., Watts, L. A., Warneke, C., and Wollny, A. G.: Characteristics, sources, and transport of aerosols measured in spring 2008 during the aerosol, radiation, and cloud processes affecting Arctic Climate (ARCPAC) Project, Atmos. Chem. Phys., 11, 2423–2453, doi:10.5194/acp-11-2423-2011, 2011.

Chen, Y. L., Kreidenweis, S. M., McInnes, L. M., Rogers, D. C., and DeMott, P. J.: Single particle analyses of ice nucleating aerosols in the upper troposphere and lower stratosphere, Geophys. Res. Lett., 25, 1391–1394, 1998.

Chung, S. H. and Seinfeld, J. H.: Global distribution and climate forcing of carbonaceous aerosols, J. Geophys. Res.-Atmos., 107, 4407, doi:10.1029/2001JD001397, 2002.

Cooke, W. F., Liousse, C., Cachier, H., and Feichter, J.: Construction of a $1^{\circ} \times 1^{\circ}$ fossil fuel emission data set for carbonaceous aerosol and implementation and radiative impact in the ECHAM4 model, J. Geophys. Res.-Atmos., 104, 22137–22162, 1999.

Cozic, J., Mertes, S., Verheggen, B., Cziczo, D. J., Gallavardin, S. J., Walter, S., Bal-

ACPD
11, 19395–19442, 2011

tensperger, U., and Weingartner, E.: Black carbon enrichment in atmospheric ice particle residuals observed in lower tropospheric mixed phase clouds, J. Geophys. Res.-Atmos., 113, D15209, doi:10.1029/2007JD009266, 2008.
Croft, B., Lohmann, U., Martin, R. V., Stier, P., Wurzler, S., Feichter, J., Posselt, R., and Ferrachat, S.: Aerosol size-dependent below-cloud scavenging by rain and snow in the ECHAM5-HAM, Atmos. Chem. Phys., 9, 4653–4675, doi:10.5194/acp-9-4653-2009, 2009.
Dana, M. T. and Hales, J. M.: Statistical aspects of washout of polydisperse aerosols, Atmos. Environ., 10, 45–50, 1976.
DelGenio, A. D., Yao, M. S., Kovari, W., and Lo, K. K. W.: A prognostic cloud water parameterization for global climate models, J. Climate, 9, 270–304, 1996.
Djupstrom, M., Pacyna, J. M., Maenhaut, W., Winchester, J. W., Li, S. M., and Shaw, G. E.: Contamination of arctic air at 3 sites during a haze event in late winter 1986, Atmos. Environ. A-Gen., 27, 2999–3010, 1993.
Doherty, S. J., Warren, S. G., Grenfell, T. C., Clarke, A. D., and Brandt, R. E.: Light-absorbing impurities in Arctic snow, Atmos. Chem. Phys., 10, 11647–11680, doi:10.5194/acp-10-11647-2010, 2010.
van Donkelaar, A., Martin, R. V., Leaitch, W. R., Macdonald, A. M., Walker, T. W., Streets, D. G., Zhang, Q., Dunlea, E. J., Jimenez, J. L., Dibb, J. E., Huey, L. G., Weber, R., and Andreae, M. O.: Analysis of aircraft and satellite measurements from the Intercontinental Chemical Transport Experiment (INTEX-B) to quantify long-range transport of East Asian sulfur to Canada, Atmos. Chem. Phys., 8, 2999–3014, doi:10.5194/acp-8-2999-2008, 2008.
Dunlea, E. J., DeCarlo, P. F., Aiken, A. C., Kimmel, J. R., Peltier, R. E., Weber, R. J., Tomlinson, J., Collins, D. R., Shinozuka, Y., McNaughton, C. S., Howell, S. G., Clarke, A. D., Emmons, L. K., Apel, E. C., Pfister, G. G., van Donkelaar, A., Martin, R. V., Millet, D. B., Heald, C. L., and Jimenez, J. L.: Evolution of Asian aerosols during transpacific transport in INTEX-B, Atmos. Chem. Phys., 9, 7257–7287, doi:10.5194/acp-9-7257-2009, 2009.
Eleftheriadis, K., Vratolis, S., and Nyeki, S.: Aerosol black carbon in the European Arctic: measurements at Zeppelin station, Ny-Alesund, Svalbard from 1998–2007, Geophys. Res. Lett., 36, L02809, doi:10.1029/2008GL035741, 2009.
Feng, J.: A 3-mode parameterization of below-cloud scavenging of aerosols for use in atmospheric dispersion models, Atmos. Environ., 41, 6808–6822, doi:10.1016/j.atmosenv.2007.04.046, 2007.
Feng, J.: A size-resolved model for below-cloud scavenging of aerosols by snowfall, J. Geo-

ACPD
11, 19395–19442, 2011

phys. Res.-Atmos., 114, D08203, doi:10.1029/2008JD011012, 2009.
Fisher, J. A., Jacob, D. J., Purdy, M. T., Kopacz, M., Le Sager, P., Carouge, C., Holmes, C. D., Yantosca, R. M., Batchelor, R. L., Strong, K., Diskin, G. S., Fuelberg, H. E., Holloway, J. S., Hyer, E. J., McMillan, W. W., Warner, J., Streets, D. G., Zhang, Q., Wang, Y., and Wu, S.: Source attribution and interannual variability of Arctic pollution in spring constrained by aircraft (ARCTAS, ARCPAC) and satellite (AIRS) observations of carbon monoxide, Atmos. Chem. Phys., 10, 977–996, doi:10.5194/acp-10-977-2010, 2010.
Fisher, J. A., Jacob, D. J., Wang, Q., Bahreini, R., Carouge, C. C., Cubison, M. J., Dibb, J. E., Diehl, T., Jimenez, J. L., Leibensperger, E. M., Meinders, M. B. J., Pye, H. O. T., Quinn, P. K., Sharma, S., van Donkelaar, A., and Yantosca, R. M.: Sources, distribution, and acidity of sulfate-ammonium aerosol in the Arctic in winter–spring, in review for Atmos. Environ., 2011.
Flanner, M. G., Zender, C. S., Randerson, J. T., and Rasch, P. J.: Present-day climate forcing and response from black carbon in snow, J. Geophys. Res.-Atmos., 112, D11202, doi:10.1029/2006JD008003, 2007.
Forster, P., Ramaswamy, V., Artaxo, P., Berntsen, T., Betts, R., Fahey, D. W., Haywood, J., Lean, J., Lowe, D. C., Myhre, G., Nganga, J., Prinn, R., Raga, G., Schulz, M., and Van Dorland, R.: Changes in atmospheric constituents and in radiative forcing, in: Climate Change 2007: The Physical Science Basis, Contribution of Working Group I to the Fourth Assessment Report of the Intergovernmental Panel on Climate Change, edited by: Solomon, S., Qin, D., Manning, M., Chen, Z., Marquis, M., Averyt, K. B., Tignor, M., and Miller, H. L., Cambridge University Press, Cambridge, UK and New York, NY, USA, 2007.
Frossard, A. A., Shaw, P. M., Russell, L. M., Kroll, J. H., Canagaratna, M. R., Worsnop, D. R., Quinn, P. K., and Bates, T. S.: Springtime Arctic haze contributions of submicron organic particles from European and Asian combustion sources, J. Geophys. Res.-Atmos., 116, D05205, doi:10.1029/2010JD015178, 2011.
Fu, T. M., Jacob, D. J., Wittrock, F., Burrows, J. P., Vrekoussis, M., and Henze, D. K.: Global budgets of atmospheric glyoxal and methylglyoxal, and implications for formation of secondary organic aerosols, J. Geophys. Res.-Atmos., 113, D15303, doi:10.1029/2007JD009505, 2008.
Fu, T. M., Jacob, D. J., and Heald, C. L.: Aqueous-phase reactive uptake of dicarbonyls as a source of organic aerosol over Eastern North America, Atmos. Environ., 43, 1814–1822, doi:10.1016/j.atmosenv.2008.12.029, 2009.
Giorgi, F. and Chameides, W. L.: Rainout lifetimes of highly soluble aerosols and gases as

ACPD
11, 19395–19442, 2011

inferred from simulations with a general-circulation model, J. Geophys. Res.-Atmos., 91, 14367–14376, 1986.
Gong, S. L., Zhao, T. L., Sharma, S., Toom-Sauntry, D., Lavoue, D., Zhang, X. B., Leaitch, W. R., and Barrie, L. A.: Identification of trends and interannual variability of sulfate and black carbon in the Canadian High Arctic: 1981–2007, J. Geophys. Res.-Atmos., 115, D07305, doi:10.1029/2009JD012943, 2010.
Hegg, D. A., Warren, S. G., Grenfell, T. C., Doherty, S. J., Larson, T. V., and Clarke, A. D.: Source attribution of black carbon in Arctic snow, Environ. Sci. Technol., 43, 4016–4021, doi:10.1021/es803623f, 2009.
Hegg, D. A., Warren, S. G., Grenfell, T. C., Doherty, S. J., and Clarke, A. D.: Sources of light-absorbing aerosol in arctic snow and their seasonal variation, Atmos. Chem. Phys., 10, 10923–10938, doi:10.5194/acp-10-10923-2010, 2010.
Held, A., Orsini, D. A., Vaattovaara, P., Tjernström, M., and Leck, C.: Near-surface profiles of aerosol number concentration and temperature over the Arctic Ocean, Atmos. Meas. Tech. Discuss., 4, 3017–3053, doi:10.5194/amtd-4-3017-2011, 2011.
Henze, D. K. and Seinfeld, J. H.: Global secondary organic aerosol from isoprene oxidation, Geophys. Res. Lett., 33, L09812, doi:10.1029/2006GL025976, 2006.
Henze, D. K., Seinfeld, J. H., Ng, N. L., Kroll, J. H., Fu, T.-M., Jacob, D. J., and Heald, C. L.: Global modeling of secondary organic aerosol formation from aromatic hydrocarbons: high- vs. low-yield pathways, Atmos. Chem. Phys., 8, 2405–2420, doi:10.5194/acp-8-2405-2008, 2008.
Hirdman, D., Burkhart, J. F., Sodemann, H., Eckhardt, S., Jefferson, A., Quinn, P. K., Sharma, S., Ström, J., and Stohl, A.: Long-term trends of black carbon and sulphate aerosol in the Arctic: changes in atmospheric transport and source region emissions, Atmos. Chem. Phys., 10, 9351–9368, doi:10.5194/acp-10-9351-2010, 2010.
Holmes, C. D., Jacob, D. J., Corbitt, E. S., Mao, J., Yang, X., Talbot, R., and Slemr, F.: Global atmospheric model for mercury including oxidation by bromine atoms, Atmos. Chem. Phys., 10, 12037–12057, doi:10.5194/acp-10-12037-2010, 2010.
Huang, L., Gong, S. L., Jia, C. Q., and Lavoue, D.: Importance of deposition processes in simulating the seasonality of the Arctic black carbon aerosol, J. Geophys. Res.-Atmos., 115, D17207, doi:10.1029/2009JD013478, 2010a.
Huang, L., Gong, S. L., Jia, C. Q., and Lavoue, D.: Relative contributions of anthropogenic emissions to black carbon aerosol in the Arctic, J. Geophys. Res.-Atmos., 115, D19208,

ACPD
11, 19395–19442, 2011

doi:10.1029/2009JD013592, 2010b.
IEA: Energy Statistics of Non-OECD Countries 2010, OECD Publishing, Paris, France, 2010.
Jacob, D. J., Crawford, J. H., Maring, H., Clarke, A. D., Dibb, J. E., Emmons, L. K., Ferrare, R. A., Hostetler, C. A., Russell, P. B., Singh, H. B., Thompson, A. M., Shaw, G. E., McCauley, E., Pederson, J. R., and Fisher, J. A.: The Arctic Research of the Composition of the Troposphere from Aircraft and Satellites (ARCTAS) mission: design, execution, and first results, Atmos. Chem. Phys., 10, 5191–5212, doi:10.5194/acp-10-5191-2010, 2010.
Jacobson, M. Z.: Strong radiative heating due to the mixing state of black carbon in atmospheric aerosols, Nature, 409, 695–697, 2001.
Jimenez, J., Jayne, J., Shi, Q., Kolb, C., Worsnop, D., Yourshaw, I., Seinfeld, J., Flagan, R., Zhang, X., and Smith, K.: Ambient aerosol sampling using the Aerodyne Aerosol Mass Spectrometer, J. Geophys. Res., 108, 8425, 2003.
Kärcher, B., Möhler, O., DeMott, P. J., Pechtl, S., and Yu, F.: Insights into the role of soot aerosols in cirrus cloud formation, Atmos. Chem. Phys., 7, 4203–4227, doi:10.5194/acp-7-4203-2007, 2007.
Kawamura, K., Kasukabe, H., and Barrie, L. A.: Source and reaction pathways of dicarboxylic acids, ketoacids and dicarbonyls in arctic aerosols: one year of observations, Atmos. Environ., 30, 1709–1722, 1996.
Klonecki, A., Hess, P., Emmons, L., Smith, L., Orlando, J., and Blake, D.: Seasonal changes in the transport of pollutants into the Arctic troposphere-model study, J. Geophys. Res.-Atmos., 108, 8367, doi:10.1029/2002JD002199, 2003.
Koch, D. and Hansen, J.: Distant origins of Arctic black carbon: a Goddard Institute for Space Studies ModelE experiment, J. Geophys. Res.-Atmos., 110, D04204, doi:10.1029/2004JD005296, 2005.
Koch, D., Bond, T. C., Streets, D., Unger, N., and van der Werf, G. R.: Global impacts of aerosols from particular source regions and sectors, J. Geophys. Res.-Atmos., 112, D02205, doi:10.1029/2005JD007024, 2007.
Koch, D., Menon, S., Del Genio, A., Ruedy, R., Alienov, I., and Schmidt, G. A.: Distinguishing aerosol impacts on climate over the past century, J. Climate, 22, 2659–2677, doi:10.1175/2008JCLI2573.1, 2009a.
Koch, D., Schulz, M., Kinne, S., McNaughton, C., Spackman, J. R., Balkanski, Y., Bauer, S., Berntsen, T., Bond, T. C., Boucher, O., Chin, M., Clarke, A., De Luca, N., Dentener, F., Diehl, T., Dubovik, O., Easter, R., Fahey, D. W., Feichter, J., Fillmore, D., Freitag, S., Ghan, S.,

ACPD
11, 19395–19442, 2011

Ginoux, P., Gong, S., Horowitz, L., Iversen, T., Kirkevåg, A., Klimont, Z., Kondo, Y., Krol, M., Liu, X., Miller, R., Montanaro, V., Moteki, N., Myhre, G., Penner, J. E., Perlwitz, J., Pitari, G., Reddy, S., Sahu, L., Sakamoto, H., Schuster, G., Schwarz, J. P., Seland, Ø., Stier, P., Takegawa, N., Takemura, T., Textor, C., van Aardenne, J. A., and Zhao, Y.: Evaluation of black carbon estimations in global aerosol models, Atmos. Chem. Phys., 9, 9001–9026, doi:10.5194/acp-9-9001-2009, 2009b.

Kondo, Y., Matsui, H., Moteki, N., Sahu, L., Takegawa, N., Kajino, M., Zhao, Y., Cubison, M. J., Jimenez, J. L., Vay, S., Diskin, G. S., Anderson, B., Wisthaler, A., Mikoviny, T., Fuelberg, H. E., Blake, D. R., Huey, G., Weinheimer, A. J., Knapp, D. J., and Brune, W. H.: Emissions of black carbon, organic, and inorganic aerosols from biomass burning in North America and Asia in 2008, J. Geophys. Res.-Atmos., 116, D08204, doi:10.1029/2010JD015152, 2011.

Kristjansson, J. E., Iversen, T., Kirkevag, A., Seland, O., and Debernard, J.: Response of the climate system to aerosol direct and indirect forcing: role of cloud feedbacks, J. Geophys. Res.-Atmos., 110, D24206, doi:10.1029/2005JD006299, 2005.

Law, K. S. and Stohl, A.: Arctic air pollution: Origins and impacts, Science, 315, 1537–1540, doi:10.1126/science.1137695, 2007.

Leibensperger, E. M., Mickley, L. J., Jacob, D. J., Chen, W.-T., Seinfeld, J. H., Nenes, A., Adams, P. J., Streets, D. G., Kumar, N., and Rind, D.: Climatic effects of 1950–2050 changes in US anthropogenic aerosols – Part 1: Aerosol trends and radiative forcing, submitted to Atmos. Chem. Phys., 2011.

Liu, H. Y., Jacob, D. J., Bey, I., and Yantosca, R. M.: Constraints from Pb-210 and Be-7 on wet deposition and transport in a global three-dimensional chemical tracer model driven by assimilated meteorological fields, J. Geophys. Res.-Atmos., 106, 12109–12128, 2001.

Liu, H. Y., Jacob, D. J., Bey, I., Yantosca, R. M., Duncan, B. N., and Sachse, G. W.: Transport pathways for Asian pollution outflow over the Pacific: interannual and seasonal variations, J. Geophys. Res.-Atmos., 108, 8786, doi:10.1029/2002JD003102, 2003.

Liu, J. F., Fan, S. M., Horowitz, L. W., and Levy, H.: Evaluation of factors controlling long-range transport of black carbon to the Arctic, J. Geophys. Res., 116, D04307, doi:10.1029/2010jd015145, 2011.

Lu, Z., Streets, D. G., Zhang, Q., Wang, S., Carmichael, G. R., Cheng, Y. F., Wei, C., Chin, M., Diehl, T., and Tan, Q.: Sulfur dioxide emissions in China and sulfur trends in East Asia since 2000, Atmos. Chem. Phys., 10, 6311–6331, doi:10.5194/acp-10-6311-2010, 2010.

ACPD
11, 19395–19442, 2011

Mao, J., Jacob, D. J., Evans, M. J., Olson, J. R., Ren, X., Brune, W. H., Clair, J. M. St., Crounse, J. D., Spencer, K. M., Beaver, M. R., Wennberg, P. O., Cubison, M. J., Jimenez, J. L., Fried, A., Weibring, P., Walega, J. G., Hall, S. R., Weinheimer, A. J., Cohen, R. C., Chen, G., Crawford, J. H., McNaughton, C., Clarke, A. D., Jaeglé, L., Fisher, J. A., Yantosca, R. M., Le Sager, P., and Carouge, C.: Chemistry of hydrogen oxide radicals (HO_x) in the Arctic troposphere in spring, Atmos. Chem. Phys., 10, 5823–5838, doi:10.5194/acp-10-5823-2010, 2010.

Matsui, H., Kondo, Y., Moteki, N., Takegawa, N., Sahu, L. K., Zhao, Y., Fuelberg, H. E., Sessions, W. R., Diskin, G., Blake, D. R., Wisthaler, A., and Koike, M.: Seasonal variation of the transport of black carbon aerosol from the Asian continent to the Arctic during the ARCTAS aircraft campaign, J. Geophys. Res.-Atmos., 116, D05202, doi:10.1029/2010JD015067, 2011.

Mc Naughton, C. S., Clarke, A. D., Freitag, S., Kapustin, V. N., Kondo, Y., Moteki, N., Sahu, L., Takegawa, N., Schwarz, J. P., Spackman, J. R., Watts, L., Diskin, G., Podolske, J., Holloway, J. S., Wisthaler, A., Mikoviny, T., de Gouw, J., Warneke, C., Jimenez, J., Cubison, M., Howell, S. G., Middlebrook, A., Bahreini, R., Anderson, B. E., Winstead, E., Thornhill, K. L., Lack, D., Cozic, J., and Brock, C. A.: Absorbing aerosol in the troposphere of the Western Arctic during the 2008 ARCTAS/ARCPAC airborne field campaigns, Atmos. Chem. Phys. Discuss., 11, 1543–1594, doi:10.5194/acpd-11-1543-2011, 2011.

McConnell, J. R., Edwards, R., Kok, G. L., Flanner, M. G., Zender, C. S., Saltzman, E. S., Banta, J. R., Pasteris, D. R., Carter, M. M., and Kahl, J. D. W.: 20th-century industrial black carbon emissions altered Arctic climate forcing, Science, 317, 1381–1384, doi:10.1126/science.1144856, 2007.

Murakami, M., Kimura, T., Magono, C., and Kikuchi, K.: Observations of precipitation scavenging for water-soluble particles, J. Meteorol. Soc. Jpn., 61, 346–358, 1983.

Nilsson, E. D. and Rannik, U.: Turbulent aerosol fluxes over the Arctic Ocean – Part 1: Dry deposition over sea and pack ice, J. Geophys. Res.-Atmos., 106, 32125–32137, 2001.

Park, R. J., Jacob, D. J., Chin, M., and Martin, R. V.: Sources of carbonaceous aerosols over the United States and implications for natural visibility, J. Geophys. Res.-Atmos., 108, 4355, doi:10.1029/2002JD003190, 2003.

Park, R. J., Jacob, D. J., Palmer, P. I., Clarke, A. D., Weber, R. J., Zondlo, M. A., Eisele, F. L., Bandy, A. R., Thornton, D. C., Sachse, G. W., and Bond, T. C.: Export efficiency of black carbon aerosol in continental outflow: global implications, J. Geophys. Res.-Atmos., 110,

ACPD
11, 19395–19442, 2011

D11205, doi:10.1029/2004JD005432, 2005.
Park, R. J., Jacob, D. J., Kumar, N., and Yantosca, R. M.: Regional visibility statistics in the United States: natural and transboundary pollution influences, and implications for the Regional Haze Rule, Atmos. Environ., 40, 5405–5423, doi:10.1016/j.atmosenv.2006.04.059, 2006.
Quinn, P. K., Miller, T. L., Bates, T. S., Ogren, J. A., Andrews, E., and Shaw, G. E.: A 3-year record of simultaneously measured aerosol chemical and optical properties at Barrow, Alaska, J. Geophys. Res.-Atmos., 107, 4130, doi:10.1029/2001JD001248, 2002.
Quinn, P. K., Shaw, G., Andrews, E., Dutton, E. G., Ruoho-Airola, T., and Gong, S. L.: Arctic haze: current trends and knowledge gaps, Tellus B, 59, 99–114, doi:10.1111/j.1600-0889.2006.00238.x, 2007.
Quinn, P. K., Bates, T. S., Baum, E., Doubleday, N., Fiore, A. M., Flanner, M., Fridlind, A., Garrett, T. J., Koch, D., Menon, S., Shindell, D., Stohl, A., and Warren, S. G.: Short-lived pollutants in the Arctic: their climate impact and possible mitigation strategies, Atmos. Chem. Phys., 8, 1723–1735, doi:10.5194/acp-8-1723-2008, 2008.
Rastigejev, Y., Park, R., Brenner, M. P., and Jacob, D. J.: Resolving intercontinental pollution plumes in global models of atmospheric transport, J. Geophys. Res., 115, D02302, doi:10.1029/2009JD012568, 2010.
Reddy, M. S. and Boucher, O.: A study of the global cycle of carbonaceous aerosols in the LMDZT general circulation model, J. Geophys. Res.-Atmos., 109, D14202, doi:10.1029/2003JD004048, 2004.
Reid, J. S., Koppmann, R., Eck, T. F., and Eleuterio, D. P.: A review of biomass burning emissions part II: intensive physical properties of biomass burning particles, Atmos. Chem. Phys., 5, 799–825, doi:10.5194/acp-5-799-2005, 2005.
Reid, J. S., Hyer, E. J., Prins, E. M., Westphal, D. L., Zhang, J. L., Wang, J., Christopher, S. A., Curtis, C. A., Schmidt, C. C., Eleuterio, D. P., Richardson, K. A., and Hoffman, J. P.: Global monitoring and forecasting of biomass-burning smoke: description of and lessons from the fire locating and modeling of burning emissions (FLAMBE) program, IEEE J. Sel. Top. Appl., 2(3), 144–162, doi:10.1109/JSTARS.2009.2027443, 2009.
Ricard, V., Jaffrezo, J. L., Kerminen, V. M., Hillamo, R. E., Sillanpaa, M., Ruellan, S., Liousse, C., and Cachier, H.: Two years of continuous aerosol measurements in Northern Finland, J. Geophys. Res.-Atmos., 107, 4129, doi:10.1029/2001JD000952, 2002.
Sharma, S., Andrews, E., Barrie, L. A., Ogren, J. A., and Lavoue, D.: Variations and sources of

ACPD
11, 19395–19442, 2011

the equivalent black carbon in the high Arctic revealed by long-term observations at Alert and Barrow: 1989–2003, J. Geophys. Res.-Atmos., 111, D14208, doi:10.1029/2005JD006581, 2006.

Shaw, G. E.: Evidence for a Central Eurasian source area of Arctic haze in Alaska, Nature, 299, 815–818, 1982.

Shaw, P. M., Russell, L. M., Jefferson, A., and Quinn, P. K.: Arctic organic aerosol measurements show particles from mixed combustion in spring haze and from frost flowers in winter, Geophys. Res. Lett., 37, L10803, doi:10.1029/2010GL042831, 2010.

Shindell, D. T., Chin, M., Dentener, F., Doherty, R. M., Faluvegi, G., Fiore, A. M., Hess, P., Koch, D. M., MacKenzie, I. A., Sanderson, M. G., Schultz, M. G., Schulz, M., Stevenson, D. S., Teich, H., Textor, C., Wild, O., Bergmann, D. J., Bey, I., Bian, H., Cuvelier, C., Duncan, B. N., Folberth, G., Horowitz, L. W., Jonson, J., Kaminski, J. W., Marmer, E., Park, R., Pringle, K. J., Schroeder, S., Szopa, S., Takemura, T., Zeng, G., Keating, T. J., and Zuber, A.: A multi-model assessment of pollution transport to the Arctic, Atmos. Chem. Phys., 8, 5353–5372, doi:10.5194/acp-8-5353-2008, 2008.

Spackman, J. R., Gao, R. S., Neff, W. D., Schwarz, J. P., Watts, L. A., Fahey, D. W., Holloway, J. S., Ryerson, T. B., Peischl, J., and Brock, C. A.: Aircraft observations of enhancement and depletion of black carbon mass in the springtime Arctic, Atmos. Chem. Phys., 10, 9667–9680, doi:10.5194/acp-10-9667-2010, 2010.

Stohl, A.: Characteristics of atmospheric transport into the Arctic troposphere, J. Geophys. Res.-Atmos., 111, D11306, doi:10.1029/2005JD006888, 2006.

Stohl, A., Berg, T., Burkhart, J. F., Fjæraa, A. M., Forster, C., Herber, A., Hov, Ø., Lunder, C., McMillan, W. W., Oltmans, S., Shiobara, M., Simpson, D., Solberg, S., Stebel, K., Ström, J., Tørseth, K., Treffeisen, R., Virkkunen, K., and Yttri, K. E.: Arctic smoke – record high air pollution levels in the European Arctic due to agricultural fires in Eastern Europe in spring 2006, Atmos. Chem. Phys., 7, 511–534, doi:10.5194/acp-7-511-2007, 2007.

Targino, A. C., Coe, H., Cozic, J., Crosier, J., Crawford, I., Bower, K., Flynn, M., Gallagher, M., Allan, J., Verheggen, B., Weingartner, E., Baltensperger, U., and Choularton, T.: Influence of particle chemical composition on the phase of cold clouds at a high-alpine site in Switzerland, J. Geophys. Res.-Atmos., 114, D18206, doi:10.1029/2008JD011365, 2009.

Tilmes, S., Emmons, L. K., Law, K. S., Ancellet, G., Schlager, H., Paris, J.-D., Fuelberg, H. E., Streets, D. G., Wiedinmyer, C., Diskin, G. S., Kondo, Y., Holloway, J., Schwarz, J. P., Spackman, J. R., Campos, T., Nédélec, P., and Panchenko, M. V.: Source contributions to

ACPD

11, 19395–19442, 2011

Northern Hemisphere CO and black carbon during spring and summer 2008 from POLARCAT and START08/preHIPPO observations and MOZART-4, Atmos. Chem. Phys. Discuss., 11, 5935–5983, doi:10.5194/acpd-11-5935-2011, 2011.

Turpin, B. J. and Lim, H. J.: Species contributions to $PM_{2.5}$ mass concentrations: revisiting common assumptions for estimating organic mass, Aerosol Sci. Tech., 35, 602–610, 2001.

Wang, Y. H., Jacob, D. J., and Logan, J. A.: Global simulation of tropospheric O_3-NO_x-hydrocarbon chemistry – Part 1: Model formulation, J. Geophys. Res.-Atmos., 103, 10713–10725, 1998.

Warneke, C., Bahreini, R., Brioude, J., Brock, C. A., de Gouw, J. A., Fahey, D. W., Froyd, K. D., Holloway, J. S., Middlebrook, A., Miller, L., Montzka, S., Murphy, D. M., Peischl, J., Ryerson, T. B., Schwarz, J. P., Spackman, J. R., and Veres, P.: Biomass burning in Siberia and Kazakhstan as an important source for haze over the Alaskan Arctic in April 2008, Geophys. Res. Lett., 36, L02813, doi:10.1029/2008GL036194, 2009.

Warneke, C., Froyd, K. D., Brioude, J., Bahreini, R., Brock, C. A., Cozic, J., de Gouw, J. A., Fahey, D. W., Ferrare, R., Holloway, J. S., Middlebrook, A. M., Miller, L., Montzka, S., Schwarz, J. P., Sodemann, H., Spackman, J. R., and Stohl, A.: An important contribution to springtime Arctic aerosol from biomass burning in Russia, Geophys. Res. Lett., 37, L01801, doi:10.1029/2009GL041816, 2010.

Warren, S. G. and Wiscombe, W. J.: Dirty snow after nuclear-war, Nature, 313, 467–470, 1985.

van der Werf, G. R., Randerson, J. T., Giglio, L., Collatz, G. J., Kasibhatla, P. S., and Arellano Jr., A. F.: Interannual variability in global biomass burning emissions from 1997 to 2004, Atmos. Chem. Phys., 6, 3423–3441, doi:10.5194/acp-6-3423-2006, 2006.

Wesely, M. L.: Parameterization of surface resistances to gaseous dry deposition in regional-scale numerical-models, Atmos. Environ., 23, 1293–1304, 1989.

Zhang, Q., Jimenez, J. L., Canagaratna, M. R., Allan, J. D., Coe, H., Ulbrich, I., Alfarra, M. R., Takami, A., Middlebrook, A. M., Sun, Y. L., Dzepina, K., Dunlea, E., Docherty, K., DeCarlo, P. F., Salcedo, D., Onasch, T., Jayne, J. T., Miyoshi, T., Shimono, A., Hatakeyama, S., Takegawa, N., Kondo, Y., Schneider, J., Drewnick, F., Borrmann, S., Weimer, S., Demerjian, K., Williams, P., Bower, K., Bahreini, R., Cottrell, L., Griffin, R. J., Rautiainen, J., Sun, J. Y., Zhang, Y. M., and Worsnop, D. R.: Ubiquity and dominance of oxygenated species in organic aerosols in anthropogenically-influenced Northern Hemisphere midlatitudes, Geophys. Res. Lett., 34, L13801, doi:10.1029/2007GL029979, 2007.

Zhang, L., Jacob, D. J., Boersma, K. F., Jaffe, D. A., Olson, J. R., Bowman, K. W., Worden, J. R.,

ACPD
11, 19395–19442, 2011

Thompson, A. M., Avery, M. A., Cohen, R. C., Dibb, J. E., Flock, F. M., Fuelberg, H. E., Huey, L. G., McMillan, W. W., Singh, H. B., and Weinheimer, A. J.: Transpacific transport of ozone pollution and the effect of recent Asian emission increases on air quality in North America: an integrated analysis using satellite, aircraft, ozonesonde, and surface observations, Atmos. Chem. Phys., 8, 6117–6136, doi:10.5194/acp-8-6117-2008, 2008.

Zhang, X. Y., Wang, Y. Q., Zhang, X. C., Guo, W., and Gong, S. L.: Carbonaceous aerosol composition over various regions of China during 2006, J. Geophys. Res.-Atmos., 113, D14111, doi:10.1029/2007JD009525, 2008b.

ACPD

11, 19395–19442, 2011

Table 1. Global GEOS-Chem emissions of carbonaceous aerosols in 2008[a].

Source	Black Carbon ($Tg\,C\,a^{-1}$)	Organic Aerosol ($Tg\,C\,a^{-1}$)
Anthropogenic[b]	7.0	14
North America (172.5–17.5° W, 24–88° N)	0.41	0.56
Europe (17.5° W–30° E, 50–88° N and 17.5° W–60° E, 33–50° N)	0.63	1.1
Russia (30–172.5° E, 50–88° N)	0.23	0.52
Asia (60–152.5° E, 0–50° N)	4.7	9.8
Rest of world	1.0	2.6
Open Fires[c]	11	84
North America (172.5–17.5° W, 24–88° N)	0.20	2.7
Europe (17.5° W–30° E, 33–88° N)	0.082	0.63
Russia (30–152.5° E, 33–60° N)	0.60	4.5
South Asia (60–152.5° E, 0–33° N)	0.77	6.1
Rest of world	9.5	70
Total	18	98

[a] Values are annual means. Different region definitions are used for anthropogenic and open fire sources.
[b] Including fossil fuel and biofuel combustion. Values are from Bond et al. (2007) but with doubling of Russian and Asian emissions (see text).
[c] From the FLAMBE inventory of Reid et al. (2009) but with major modifications for Russian and Southeast Asian sources as described in the text.

ACPD
11, 19395–19442, 2011

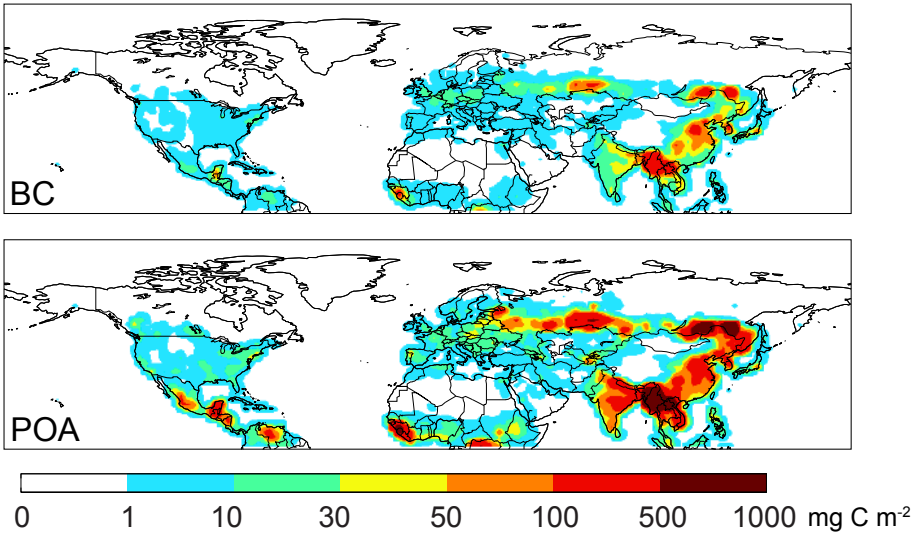

Fig. 1. GEOS-Chem emissions of black carbon (BC) and primary organic aerosol (POA) in April 2008. Annual regional totals are in Table 1.

ACPD
11, 19395–19442, 2011

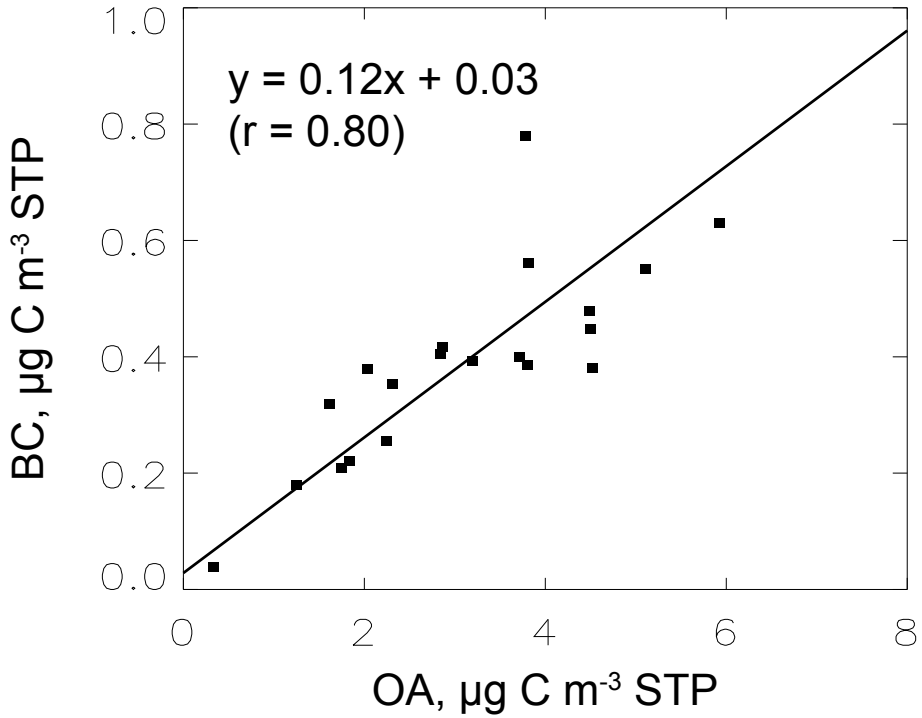

Fig. 2. Scatterplot of BC vs. OA concentrations in fire plumes diagnosed by $[CH_3CN] > 200$ ppt for the ensemble of ARCTAS DC-8 flights (1–19 April 2008). STP refers to standard conditions of temperature and pressure (273 K, 1 atm) so that μg C m^{-3} STP is a mixing ratio unit. The reduced-major-axis (RMA) regression is shown by the solid line and the corresponding equation is given inset.

ACPD
11, 19395–19442, 2011

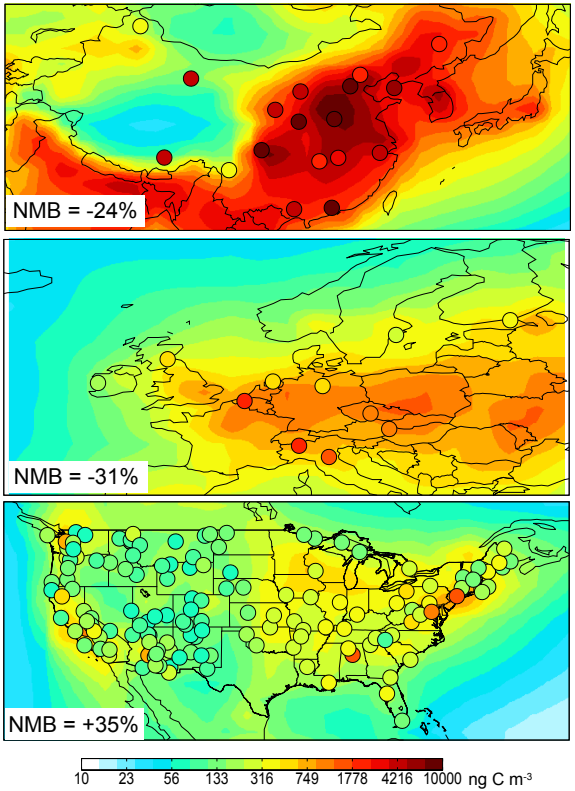

Fig. 3. Annual mean surface air concentrations of BC aerosol in China, Europe, and the US. Model results for 2008 (solid contours) are compared to observations (circles). Observations are from Zhang et al. (2008) in China for 2006, from the EMEP network in Europe for 2002–2003 (http://tarantula.nilu.no/projects/ccc/emepdata.html), and from the IMPROVE network in the US for 2008 (http://vista.cira.colostate.edu/improve/Data/IMPROVE/AsciiData.aspx). Normalized mean bias (NMB) statistics for each region are shown inset.

ACPD
11, 19395–19442, 2011

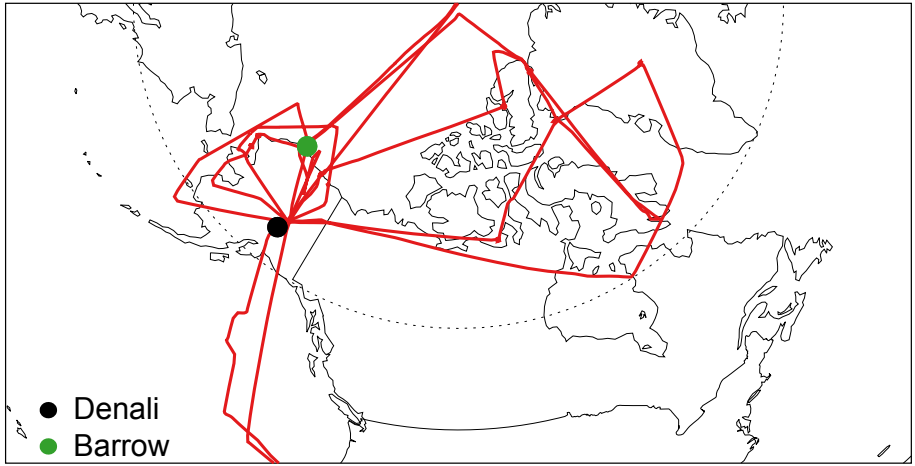

Fig. 4. DC-8 flight tracks during the April 2008 ARCTAS campaign (red lines). Long-term monitoring sites for BC at Barrow and Denali are also indicated.

ACPD
11, 19395–19442, 2011

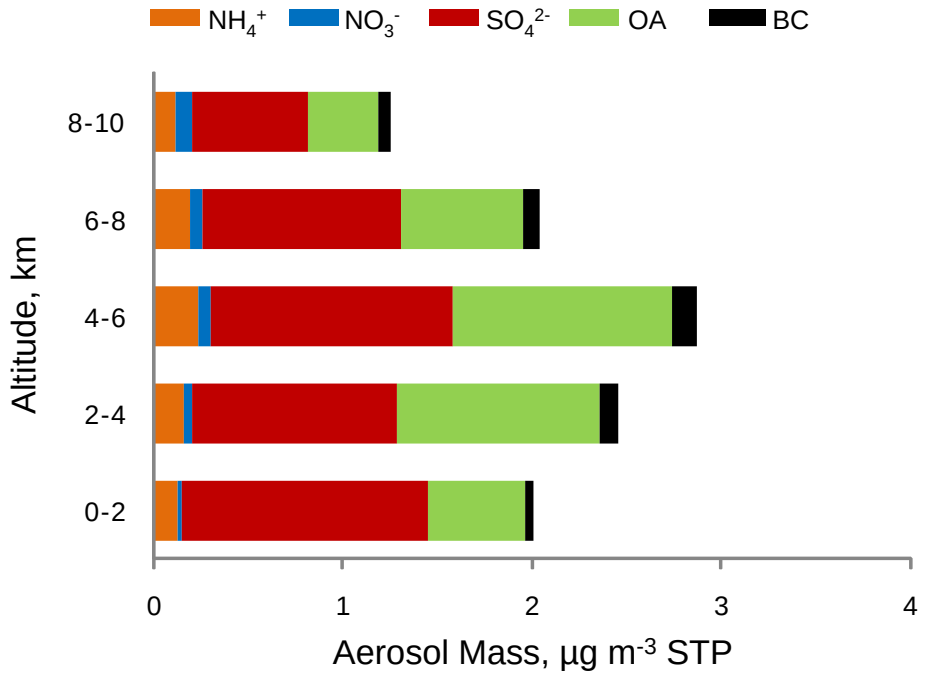

Fig. 5. Fine aerosol composition observed along the ARCTAS DC-8 flight tracks (1–19 April 2008), averaged over 2-km altitude bins. The averaging excludes data collected south of 60° N, in stratospheric air, and in biomass burning plumes (see text).

ACPD
11, 19395–19442, 2011

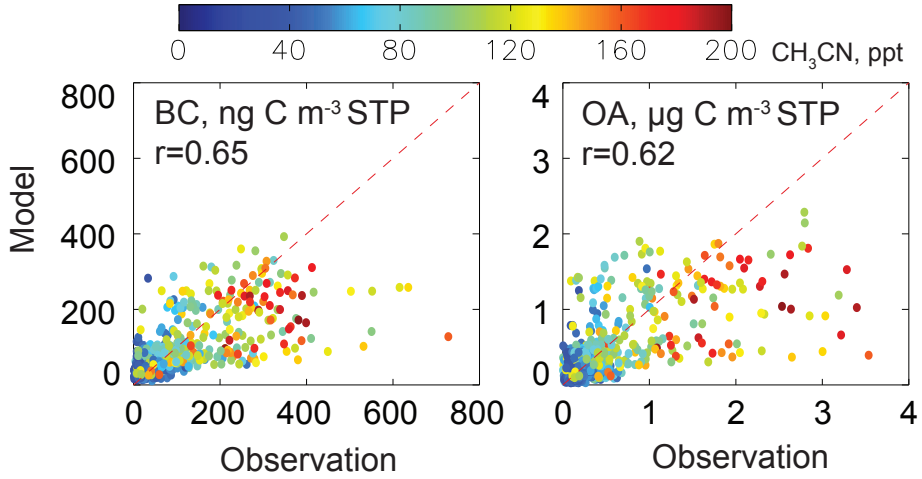

Fig. 6. Scatterplots of simulated vs. observed BC and OA concentrations along the DC-8 flight tracks during ARCTAS (1–19 April 2008). Colors indicate the corresponding concentrations of CH_3CN, a tracer of biomass burning. The 1:1 line is also shown.

ACPD
11, 19395–19442, 2011

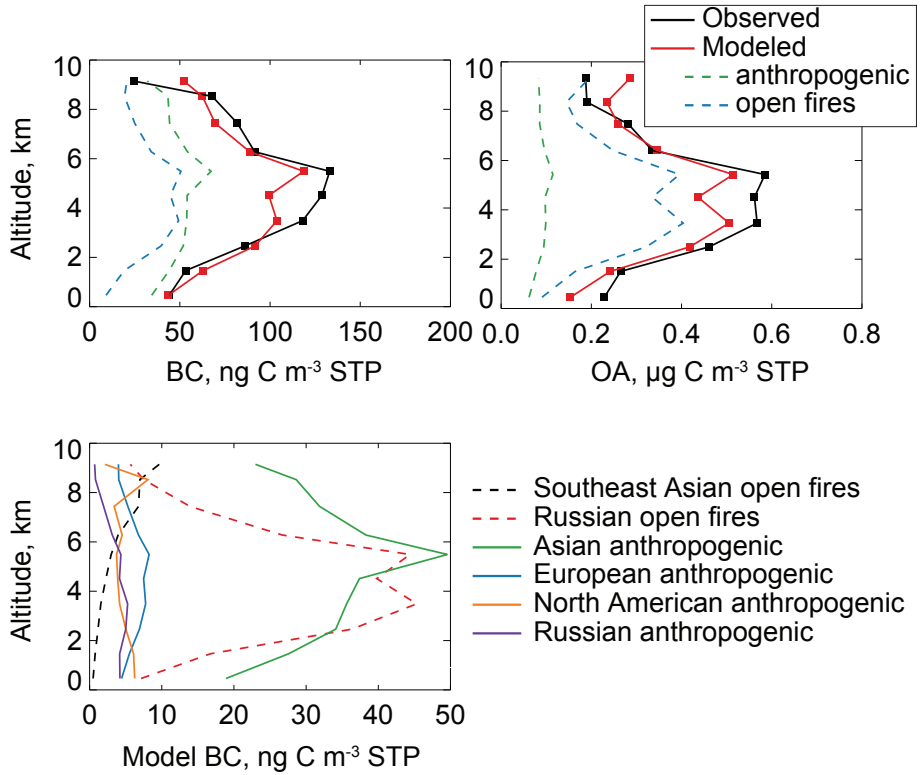

Fig. 7. Mean vertical profiles of BC and OA concentrations along the DC-8 flight tracks in ARCTAS (1–19 April 2008), averaged over 1-km altitude bins. The top panels compare observations to GEOS-Chem and separate the model contributions from anthropogenic and open fire sources. The bottom panel further separates model BC contributions by source regions. Anthropogenic sources include fossil fuel and biofuel combustion.

ACPD
11, 19395–19442, 2011

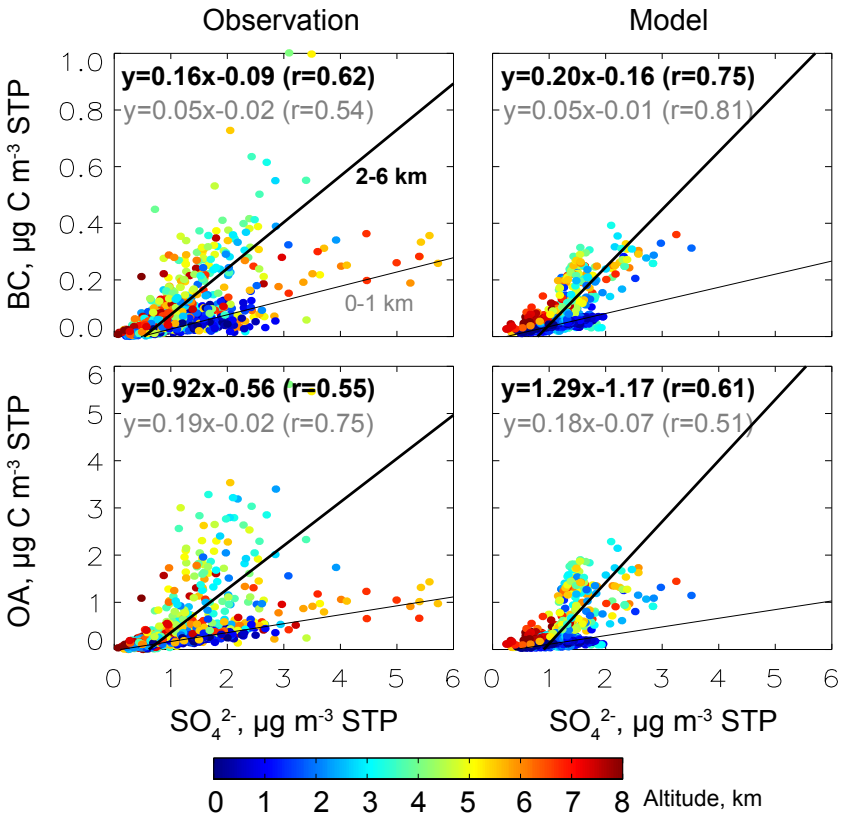

Fig. 8. Scatterplots of BC and OA vs. sulfate (SO_4^{2-}) concentrations in ARCTAS. Observations from the DC-8 aircraft (left panels) are compared to model values sampled along the aircraft flight tracks (right panels). Individual points are colored by altitude. Reduced-major-axis (RMA) regression statistics and linear fits are shown in thin black for near-surface data (<1 km) and in thick black for mid-tropospheric data (2–6 km).

ACPD
11, 19395–19442, 2011

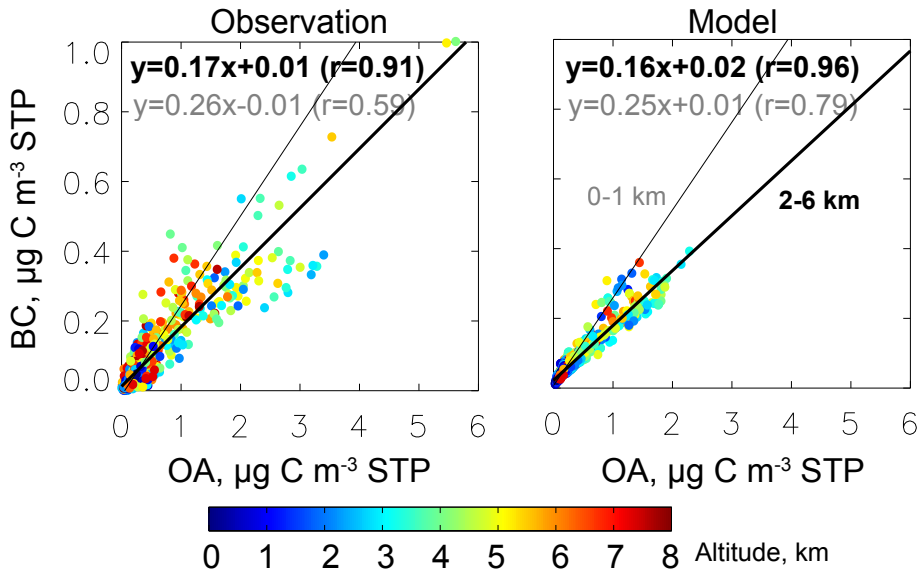

Fig. 9. Same as Fig. 8 but for BC vs. OA concentrations in ARCTAS.

ACPD
11, 19395–19442, 2011

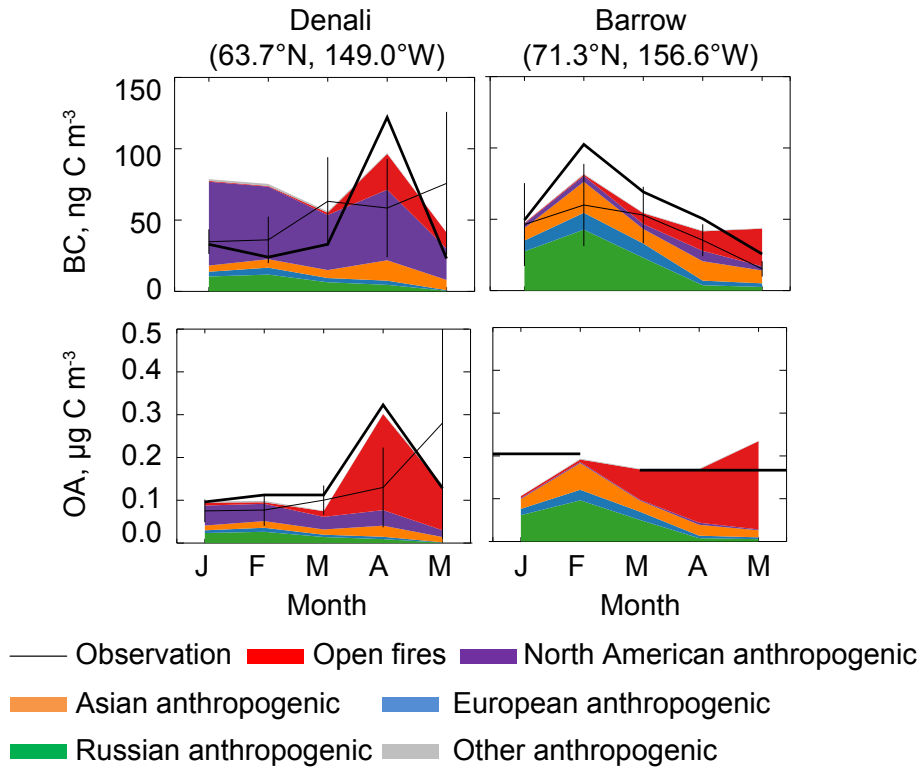

Fig. 10. Seasonal variation of BC and OA surface air concentrations at Denali and Barrow in Alaska. The thick black lines are monthly mean observations for 2008. The thin black lines are monthly mean observations for 2002–2008 with vertical bars representing interannual standard deviations. The thick line for OA at Barrow represents seasonal mean concentrations in November 2008–February 2009 and March–June 2008 from Shaw et al. (2010). Additive model contributions from different sources in the 2008 simulation are shown in color.

ACPD
11, 19395–19442, 2011

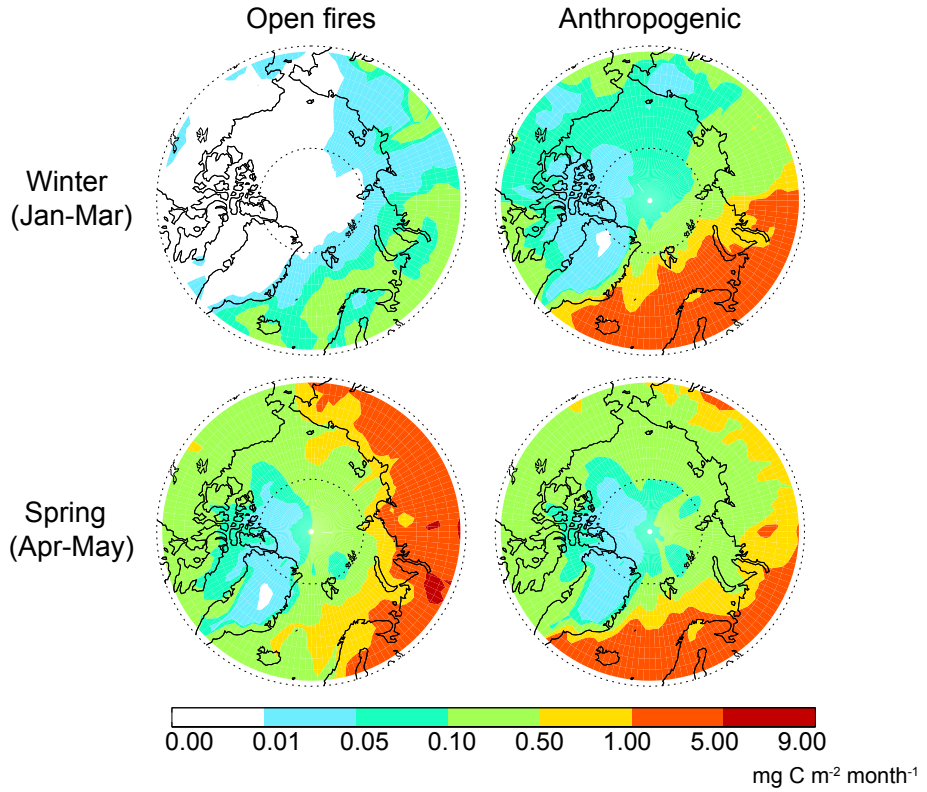

Fig. 11. Contributions of open fire and anthropogenic (fuel combustion) sources to the BC deposition flux in GEOS-Chem for winter and spring 2008.

ACPD
11, 19395–19442, 2011

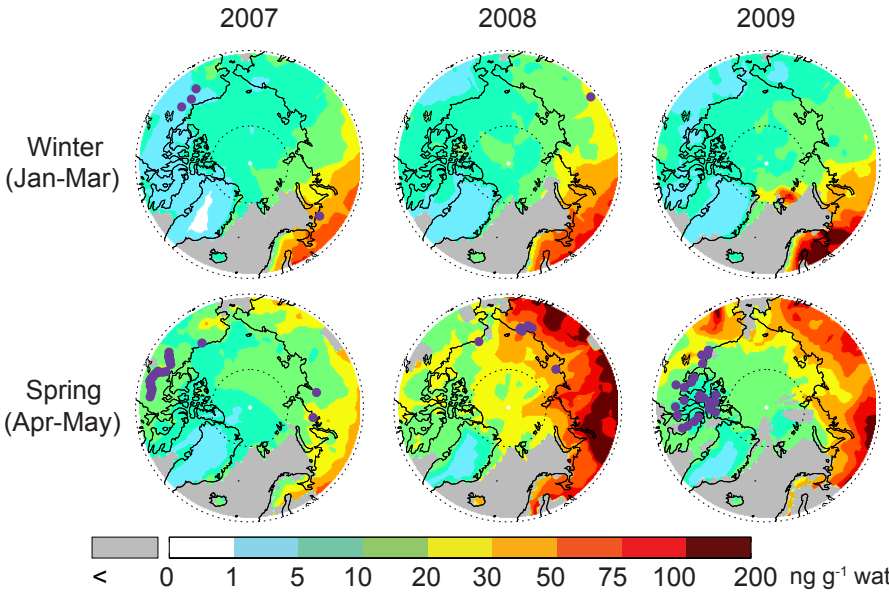

Fig. 12. Simulated BC content of Arctic snow in winter and spring 2007–2009. Snow-free areas are shown in gray. Purple circles indicate snow sampling sites from Doherty et al. (2010) for the corresponding years and seasons.

ACPD
11, 19395–19442, 2011

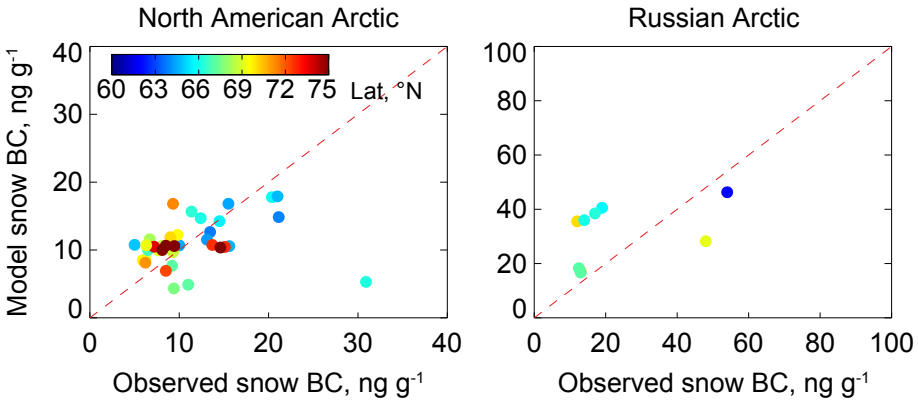

Fig. 13. Scatterplots of simulated vs. observed BC content in snow for North American and Russian Arctic sites in March–May 2007–2009 (Fig. 12). Observations from Doherty et al. (2010) are averaged over model grid squares, and model results are sampled for the month and year of observations. The data are colored by latitude. Also shown is the 1:1 line.

ACPD
11, 19395–19442, 2011

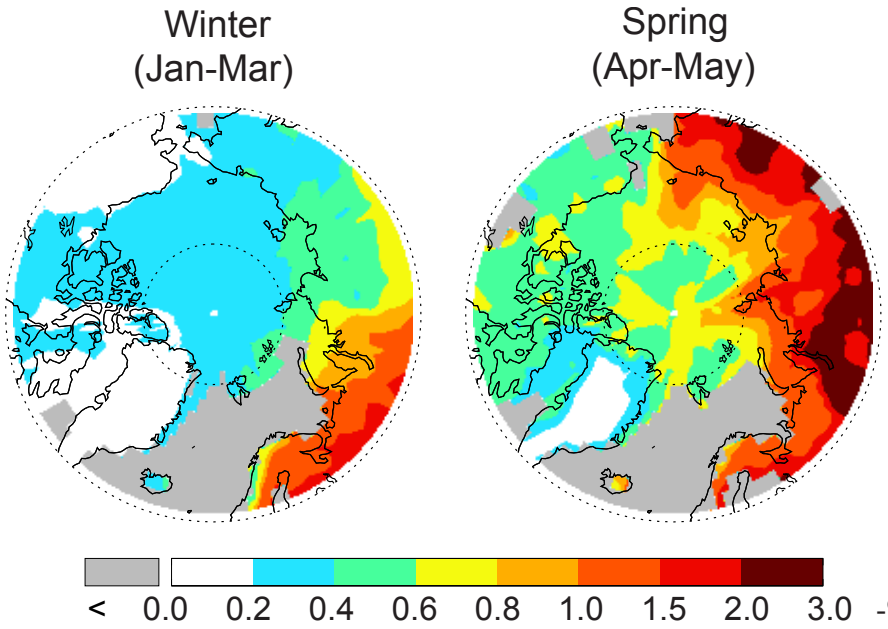

Fig. 14. Model decreases in snow albedo due to BC deposition in the Arctic (>60° N) in winter and spring 2008. Snow-free areas are shown in gray.

ACPD
11, 19395–19442, 2011